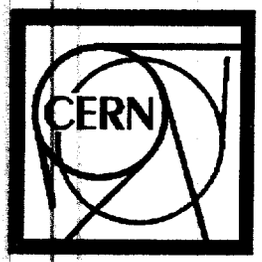

Letter of Intent
CERN/LHCC 97-49
LHCC / I 11
15 Aug. 1997

European Organization for Nuclear Research
CH-Geneva 23
Switzerland

TOTEM

Total Cross Section, Elastic Scattering and Diffraction Dissociation at the LHC

Collaboration

W. Kienzle, CERN, Geneva, Switzerland
M. Bozzo, Università di Genova and Sezione INFN, Genova, Italy
M. Buénerd, Institut des Sciences Nucléaires, IN2P3/CNRS, Grenoble, France
Y. Muraki, University of Nagoya, Nagoya, Japan
J. Bourotte and M. Haguenauer, École Polytechnique, IN2P3/CNRS, Palaiseau, France
G. Sanguinetti, Sezione INFN Pisa, Pisa, Italy
G. Matthiae, Università di Roma II and Sezione INFN, Roma, Italy
A. Faus-Golfe and J. Velasco, IFIC, Centro Mixto Universitat de València-CSIC, València, Spain

Foreword by André Martin, CERN, Geneva, Switzerland

Spokesman : Giorgio Matthiae – Technical Co-ordinator : Werner Kienzle

CERN/LHCC 97-49
LHCC/I 11
15 August 1997

Letter of Intent

Total Cross Section, Elastic Scattering and Diffraction Dissociation at the LHC

The **TOTEM** Collaboration [1]

W.Kienzle, CERN, Geneva, Switzerland
M.Bozzo, Università di Genova and Sezione INFN, Genova, Italy
M. Buénerd, Institut des Sciences Nucléaires, IN2P3/CNRS, Grenoble, France
Y.Muraki, University of Nagoya, Nagoya, Japan
J.Bourotte and M.Haguenauer, Ecole Polytechnique, IN2P3/CNRS, Palaiseau, France
G.Sanguinetti, Sezione INFN Pisa, Pisa, Italy
G.Matthiae, Università di Roma II and Sezione INFN, Roma, Italy
A.Faus-Golfe and J.Velasco, IFIC, Centro Mixto Universitat de Valencia-CSIC, Valencia, Spain

Foreword by André Martin, CERN, Geneva, Switzerland

Abstract

We propose an experiment to measure the total cross section, elastic scattering and diffraction dissociation at the LHC. Our aim is to obtain accurate information on the basic properties of proton-proton collisions at the maximum accelerator energy. For these measurements, we have to detect particles emitted in the very forward region.

The experimental method and the techniques which are involved are very special and quite different from those used in the large general purpose detectors. Therefore we believe that these measurements should be performed by a dedicated experiment.

Our first objective is the measurement of the total cross section. This can be done with a limited amount of running time at low luminosity possibly during the early running-in phase of the accelerator. No special infrastructure is required; the cost of the apparatus is quite modest.

Spokesman : G.Matthiae *Technical Coordinator*: W.Kienzle

[1] TOTEM is a acronym for TOTal and Elastic Measurement.
The present list of authors includes only the representatives of the collaborating institutions. The actual number of collaborators will be expanded in due course as the project develops.

Contents

Foreword:

WHY SHOULD ONE MEASURE PROTON-PROTON ELASTIC SCATTERING AND TOTAL CROSS-SECTION AT THE LHC

André MARTIN

Theoretical Physics Division, CERN
CH - 1211 Geneva 23

To the participants of the TOTEM collaboration, it seems obvious that if one has the highest possible proton-proton centre-of-mass energy in the world (except for cosmic rays) at the LHC one must take advantage of this and measure the proton-proton elastic scattering and, at the same time, the total cross-section, using the optical theorem or some other method.

However, some physicists might object that such an experiment will neither test the standard model, in the sense that it is not possible to compare the measurement with a calculation ab initio, from the value of Λ_{QCD}, the number of flavours and the masses of the quarks, nor constitute a window to look for phenomena beyond the Standard Model. Concerning the former point let me say that it is as if one decided not to measure the boiling temperature of water as a function of pressure because one cannot confront it with a calculation using only as input data the mass of the proton, the mass of oxygen, the mass of the electron and the fine structure constant. The proton-proton total cross-section is first of all something we have to know, the most down to earth reason being to normalize the cross-sections for supposedly "interesting" processes. In fact we already need now an estimate of this cross-section, because we want to know how many collisions will take place when two protons bunches cross inside the LHC and we want to have a system of detection able to sustain that. Present estimates are based on measurements of total cross-sections and real parts, combined with some simplicity assumptions. In 1984, C. Bourrely and A.M. [1] gave rather crude limits for total cross-sections at 1.8 TeV (previously scheduled energy) of 110 $\pm$ 20 mb. A more refined estimate, by the group UA4/2, taking into accounts more recent measurements, such as the precise measure of the real part at the SP$\bar{\text{P}}$S collider (the corresponding measurement at the Tevatron is too inaccurate to be useful!), gives, at 14 TeV, 109 mb $\pm$ 8 mb [2]. This, however, does not replace a direct accurate measurement, which avoids all uncontrollable uncertainties, like the postulate

that at these high energies the difference between pp and $p\bar{p}$ scattering in negligible (absence of "odderon") and the validity of dispersion relations. Precisely, the belief that proton-proton scattering is not going to reveal new physics is not necessarily correct. New physics could be revealed, as we shall see, by a violation of dispersion relations, which itself could be due to the appearance of a fundamental length in the theory (I am not speaking of the Planck length!). On the origin of this fundamental length, I know at present two possibilities: the existence of extra compact dimensions for the spacetime, as advocated by N.N. Khuri [3], or the discretisation of space due to quantum groups as proposed very recently by J. Wess [4] (one of the inventors of supersymmetry!). This will be discussed later.

If there is no calculation ab initio, there are several reasonable models describing proton-proton scattering and these are worth comparing with experiment. A subset of these models is the Cheng-Wu model [5], which became the Cheng-Wu-Walker model [6], eventually fully exploited by Wu, Bourrely and Soffer [7].

The Donnachie-Landshoff model [8], which is only ment to describe pp scattering at presently available energies, and probably at the LHC, but cannot describe the asymptotic energy domain because it violates "sacred" bounds.

The Kaidalov-Ter Martyrosian model [9], based on a supercritical Pomeron. I shall not discuss the critical Pomeron case, which is very well described by Moshe Moshe [10], but has the unpleasant feature that the elastic to total cross-section is decreasing, in disagreement with present experiments.

As a list of features to be looked at in elastic pp scattering, we can take the one of G. Matthiae [11]

- total cross-sections and real part
- the forward peak
- the ratio of elastic to total cross-sections
- the dip shoulder region and the large momentum transfer region.

Concerning the total cross-section, we know that it should satisfy the Froissart-Martin bound [12]

$$\sigma_T < \frac{\pi}{m_\pi^2} \ (\ln s)^2$$

we also know that the constant in front of $\log^2$ is by construction a wild overestimate. Whether the bound is qualitatively saturated is an important issue raising lots of discussions. In the paper of Augier et al. [2] it is argued that the best fit is given by $(\log s)^\gamma$, γ compatible with 2. In the Bourrely-Cheng-Soffer-Walker-Wu model, as well as in the supercritical Pomeron model of Kaidalov and Ter Martyrosian [9] this comes out naturally. For the time being, evidence is indirect, using dispersion relations together with the assumption that $\sigma_{p\bar{p}} - \sigma_{pp}$ decreases like $s^{-\nu}$, ν close to $1/2$ [13]. One may hope that the situation will be improved if the disagreement between CDF and E710 on the total cross-section [14] is resolved and if sufficiently accurate and trustable measurements of ρ, the ratio of the real part to the imaginary part in the forward direction are done at the tevatron. Also a measurement of σ_{pp} at RHIC would be of a great help

if sufficiently accurate. But this does not dispense us from making a direct measurement of σ_T at the LHC, trying to answer the question whether the Froissart-Martin bound is qualitatively saturated, at an energy where one can distinguish different powers of log, and testing dispersion relations which is something absolutely crucial as we shall see later. The non-saturation of the Froissart bound would constitute, to my own eyes, a miraculous dynamical cancellation extremely interesting. As for the measurement of ρ, at LHC, it would be of a great value, if one corrects for the almost unavoidable variation of $\rho(s,t)$ as a function of the momentum transfer that I predicted recently because of the occurrence of a zero of the real part [15]. This zero, in most models, is fortunately sufficiently far away from the interference region.

Next comes the diffraction peak for which one predicts an increasing slope with energy. In presently available data, Nicolescu and his friends see indications of oscillations which should necessarily occur at asymptotic energies if the Froissart-Martin bound is saturated [16]. Whether they do occur now or constitute an artifact due to systematic errors is unclear, but one should certainly look for that at the LHC, and if they do, it would be "new physics of the second kind", i.e., an unexpected phenomenon which may nevertheless have its explanation inside the Standard Model (like high T_c superconductors for whom we believe that an explanation will be found some day within the framework of ordinary forces and ordinary quantum mechanics). A careful analysis of the diffraction peak might allow to construct the corresponding profile function in impact parameter space and allow to test the recent theory of G. Parisi [17], according to which, after a plateau of length log s, one has a tail of width $(\log s)^{1/3}$.

Next, but interrelated because elastic scattering is dominated by the diffraction peak, comes the ratio of elastic to total cross-sections. It is known that in the ISR range, this ratio seemed to be constant, independent of energy, a fact which suggests a regime of "geometrical scaling", but that the SP$\bar{\text{P}}$S and Tevatron data indicate that it is rising. This is in complete agreement with the model of Wu and collaborators [7], Kaidalov-Ter Martyrosian [9] and Donnachie-Landshoff [8] who have an effective Pomeron intercept above unity. The asymptotic prediction of Wu and collaborators is that $\sigma_{el}/\sigma_T \to 1/2$, i.e., that the proton becomes a black disk (with radius increasing like log s). Though this is very remote, the trend is predicted to be visible at LHC, with a predicted ratio $\sigma_{el}/\sigma_T \simeq 0.28$ [1] to be compared to 0.215 at the SP$\bar{\text{P}}$S, and, taking a questionable average of E710 and CDF, 0.244 at the Tevatron.

Next we come to the dip-shoulder region. At the ISR a beautiful dip was observed in pp collisions, moving towards $t = 0$ as energy increases with an average location at $t = -1.2$ GeV^2. In $p\bar{p}$ collisions, limited experimental evidence seemed to indicate that the dip was replaced by a shoulder, and it seemed also the case at the SP$\bar{\text{P}}$S. Wu and collaborators predict a continuously moving dip [7], while Donnachie and Landshoff [5] predict a deeper dip for pp and a shoulder for $p\bar{p}$ because in their model, they have a kind of weak odderon due to three gluon exchange. The LHC, with its very high luminosity, is an ideal instrument to study this region where the counting rate is normally low. One could even see secondary structures that no other machine could get, and study the energy dependence of very large momentum transfer scattering.

In summary, there is a list of very interesting observations to make at the LHC.

Now I would like to turn to tests of dispersion relations and possible new physics. The

tests of dispersion relations will be much more severe if σ_T and hopefully ρ are measured at the LHC, but also if the accuracy of measurements at presently accessible energies is improved. It is regrettable that it will be impossible to switch from pp to $p\bar{p}$ to test the asssumption – about which Nicolescu and collaborators [18] raised some doubt – that the cross-section differences become negligible at high energy. This would have been technically feasible according to CERN engineers, but is financially impossible. New results on the pp cross-section from RHIC might allow a comparison between pp and $p\bar{p}$ at a lower energy.

Now, what comes into a dispersion relation is the fact that

i) the scattering amplitude is analytic in a twice cut plane,

ii) in the complex plane it is polynomially bounded [19]. In fact the number of subtractions is at most 2 [20].

i) and ii) have been derived from the axioms of local field theory. Most theoreticians agree that even if the theory was not strictly local, i.e., if there was in some way a fundamental length (I exclude the Planck length, too small to bother us at 14 TeV), i) would survive but ii), i.e., the polynomial boundedness, might disappear. Following Nick Khuri in his La Thuile and Blois talks of 1994-95 [3], there could be a fundamental length R, and if so, dispersion relations should be altered by putting in a convergence factor which would mix the real and imaginary parts of the amplitude. Then, quite sizeable deviations from "normal" dispersion relations could appear, in fact may be already at the Tevatron. Such a fundamental length could come from some extra internal compact dimensions, like in the Model of Antoniadis et al. [21], where it is responsible for the breakdown of supersymmetry. Another completely different origin for a fundamental length would be the one proposed by Julius Wess [4]. If quantum groups play a role in particle physics they will lead to a discretisation of space and hence, again, a fundamental length. As pointed out by Nick Khuri, it would be possible for the first time to see distances smaller than those obtained from precise QED tests.

In conclusion, testing dispersion relations at the LHC might be much more than a routine check, but may come out on something big. In my opinion, the outcome of the test is infinitely less predictable than that of the one consisting in comparing the energy levels of hydrogen and antihydrogen, in which TCP and therefore also locality is tested (an approved experiment!).

References

[1] C. Bourrely and A. Martin, Proceedings of the ECFA-CERN Workshop. Lausanne and Geneva 1984, ECFA 84/85, CERN 84-10, p. 323.

[2] C. Augier et al., *Phys.Lett.* **316B** (1993) 448.

[3] N.N. Khuri in Proceedings of the Rencontres de la Vallée d'Aoste, March 1994, M. Greco editor, Editions Frontières 1994, p. 701, and in "Frontiers in Strong Interactions", Pro-

ceedings of the VIIth "Rencontres de Blois", P. Chiappetta, M. Haguenauer and J. Tran Thanh Van eds., Editions Frontières, Gif-sur-Yvette (1996), p. 463.

[4] J. Wess, Talk given at the International Workshop on Mathematical Physics, in honour of Walter Thirring, Kiev, May 1997, to appear in the Proceedings.

[5] H. Cheng and T.T. Wu, *Phys.Rev.Lett.* **24** (1969) 666.

[6] H. Cheng, J.K. Walker and T.T. Wu, *Phys.Lett.* **B44** (1973) 112.

[7] C. Bourrely, J. Soffer and T.T. Wu, *Nucl.Phys.* **B247** (1984) 15; *Z.Phys.* **37** (1988) 369; *Phys.Lett.* **B252** (1990) 287.

[8] A. Donnachie and P.V. Landshoff, *Z.Phys.* **C2** (1979) 55; *Nucl.Phys.* **B231** (1983) 189; *Nucl.Phys.* **B267** (1986) 690.

[9] See, for instance: A.B. Kaidalov, *Physics Reports* **50** (1977) 157.

[10] M. Moshe, *Physics Reports* **37C** (1978) 257.

[11] G. Matthiae, *Rep.Prog.Phys.* **57** (1994) 743.

[12] M. Froissart, *Phys.Rev.* **123** (1961) 1053;
A. Martin, *Nuovo Cimento* **42** (1966) 930;
L. Łukaszuk and A. Martin, *Nuovo Cimento* **47A** (1967) 65.

[13] See, for instance, A. Martin, in Proceedings of the Rencontres de la Vallée d'Aoste, March 1994, M. Greco editor, Editions Frontières 1994, p. 407.

[14] see Ref. [11], for instance.

[15] A. Martin, CERN Preprint TH. 97-23, to appear in Phys.Lett. B.

[16] P. Gauron, B. Nicolescu and O.V. Selyugin, *Phys.Lett.* **B397** (1997) 305.

[17] G. Parisi, Talk given at the meeting "Discrete Structures and Physics", on the occasion of Tullio Regge's 65th Birthday, Torino, June 1997.

[18] L. Łukaszuk and B. Nicolescu, *Nuovo Cimento Letters* **8** (1973) 405;
P. Gauron, E. Leader and B. Nicolescu, *Phys.Rev.Lett.* **B54** (1985) 2656 and **55** (1985) 639;
D. Bernard, P. Gauron and B. Nicolescu, *Phys.Lett.* **B199** (1987) 125.

[19] H. Epstein, V. Glaser and A. Martin, *Commun.Math.Phys.* **13** (1969) 257.

[20] Y.S. Jin and A. Martin, *Phys.Rev.* **135B** (1964) 1377.

[21] I. Antoniadis, C. Muñoz and M. Quiros, *Nucl.Phys.* **B303** (1988) 407.

1 Introduction

At the time of the Evian Meeting on the LHC programme in 1992 we presented an "Expression of Interest"[1] to perform an experiment on "Total cross section, elastic scattering and diffraction dissociation at LHC".
Our experimental programme consists of the following measurements :

1) The **total cross section** with absolute error of about 1 mb.

2) Elastic scattering in the largest possible interval of momentum transfer from the Coulomb region ($-t \sim 5 * 10^{-4}\text{GeV}^2$) up to at least $-t \sim 10$ GeV^2.

3) The process of **diffraction dissociation**

$$p + p \rightarrow p + X$$

The experiment does not require intense beams and very high luminosities. It is therefore suited for running at the beginning of LHC operation. Our first objective is to measure the total cross section at the earliest stage of the machine operation.

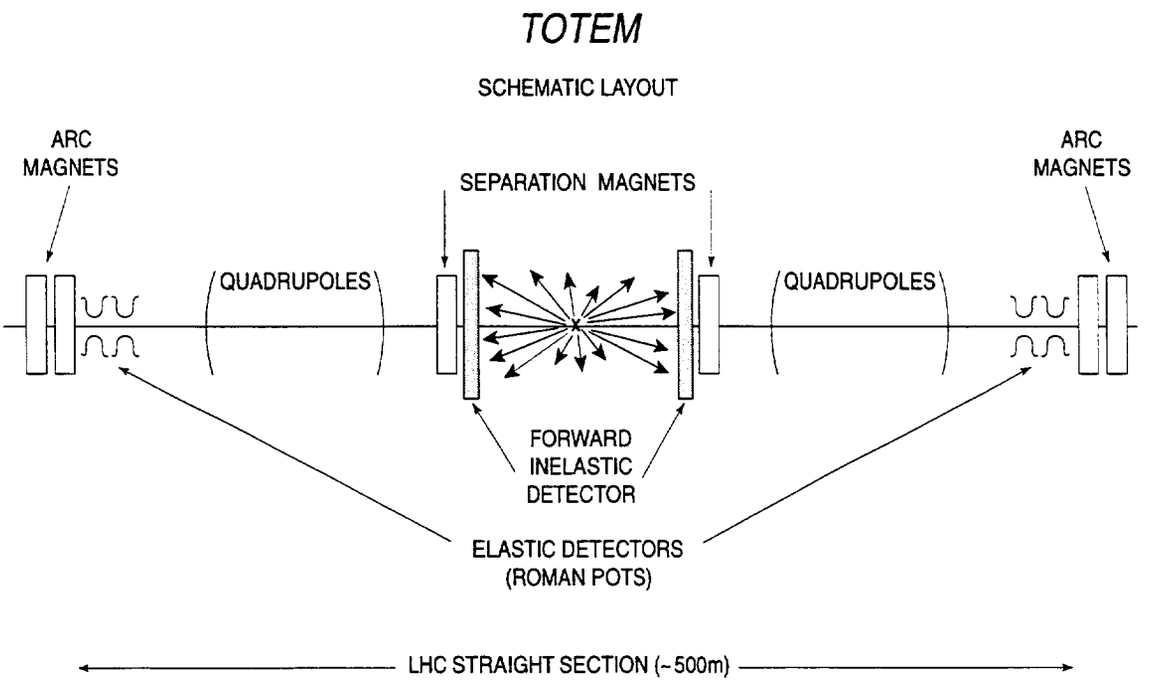

Figure 1: Sketch of the experimental apparatus of TOTEM

A sketch of the experimental apparatus is shown in Fig.1. It consists of:
1) *Elastic scattering detectors* of small size and high spatial resolution, placed symmetrically on both sides of the crossing region. They will be improved and miniaturised versions of the "Roman pots" used at the lower energy machines. They

will be placed in the vertical plane where the beam is generally more stable and will approach the beam from above and below. The "Roman pots" will also be used to detect the proton which is scattered quasi-elastically in diffraction dissociation.

2) *A forward inelastic detector* covering, on both sides of the crossing, an interval of more than three pseudo-rapidity units ($5 \leq \eta \leq 8.5$) close to the beam rapidity ($y_{beam} = 9.6$), with full azimuthal acceptance. This detector will be used for the measurement of the inelastic rate including events of diffractive type. An electromagnetic calorimeter near the forward direction will complement the "inelastic detector".

Our apparatus will detect particles in the forward or very forward cone, an angular region not covered by the other large detectors which have been proposed. At high energy, elastic scattering is confined to such small angles that the measurement is possible only in a special insertion with high-β optics. The forward inelastic detector is needed only for the measurement of the total cross section and diffraction dissociation.

The whole equipment is of small size in the direction transverse to the beam. It will be placed far away from the crossing point and will easily fit inside the existing tunnel without any need for civil engineering.

In 1993 following a request of the LHC Committee on the machine implications of TOTEM, we prepared a short document[2] discussing the main requirements on the insertion. A feasibility study of the high-β optics was then performed by machine experts and a tentative insertion was designed[3]. Our own evaluation[4] of this insertion in terms of the parameters which are relevant for the physics measurement was afterwards presented to the LHCC.

In November 1995 a discussion on the physics motivation of TOTEM was presented at the "Open LHCC Meeting on Further Physics Topics".

In this document we formally submit a Letter of Intent to the LHC Committee discussing the physics programme, the experimental method and also some preliminary technical options.

2 The Physics Programme

In this Section we briefly review the experimental information available from present high-energy accelerators. We shall also mention theoretical expectations and predictions by existing models.

2.1 The Total Cross Section

A compilation of the total cross sections for proton-proton and proton-antiproton collisions at high energy is shown in Fig.2.

Data on both pp and $\bar{p}p$ exist only up to the maximum energies of the ISR ($\sqrt{s} =$ 62 GeV). At these energies the pp and $\bar{p}p$ cross sections tend to approach each other.

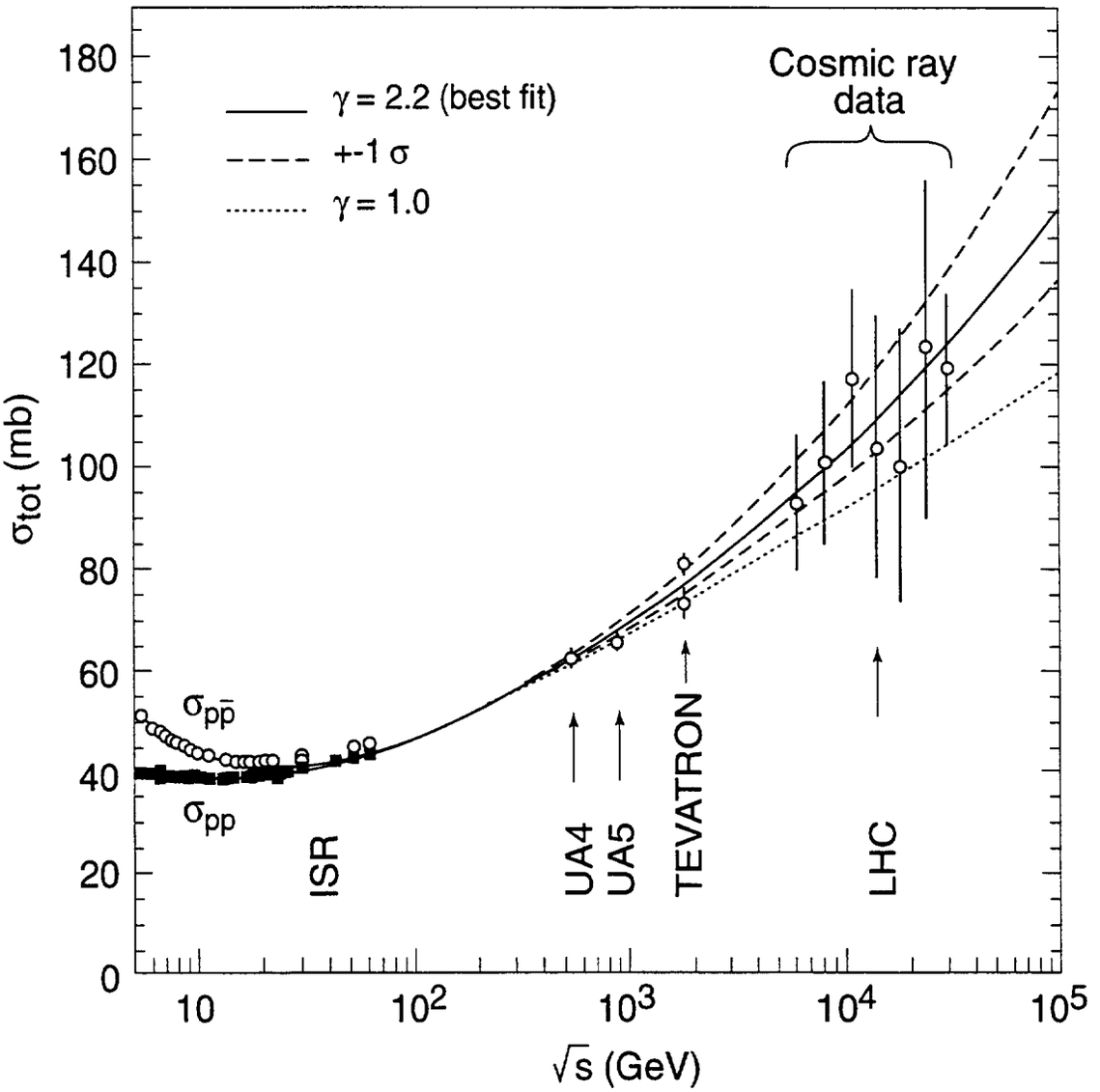

Figure 2: The total cross section for $\bar{p}p$ and pp scattering is shown together with the prediction of the dispersion relations fit of ref.[5]. The best fit (solid line) corresponds to γ =2.2. The region of uncertainty is delimited by the dashed lines. The result obtained with $\gamma = 1$ is shown as a dotted line. The expected uncertainty of the TOTEM measurement at LHC will appear in this plot as large as the data point itself.

At higher energies we only have data for $\bar{p}p$ (from the SPS and Fermilab Colliders) but results on pp collisions at $\sqrt{s} = 500$ GeV are soon expected from RHIC.

A question which has been debated for a long time is whether σ_{tot} increases as $\log s$ or $(\log s)^2$. The solid line in Fig.2 represents the result of a recent dispersion relation fit[5] which is based on measurements of σ_{tot} and of the parameter ρ (ratio of the real to the imaginary part of the forward amplitude) in the c.m.s. energy interval $5 \leq \sqrt{s} \leq 546$ GeV. The high-energy dependence of the total cross section was described by the term $(\log s/s_0)^\gamma$ with $s_0 = 1$ GeV^2. The best fit gives $\gamma = 2.2 \pm 0.3$.

The experimental data on the higher energy range and the results of the fit of ref.[5] are listed in Table 1 together with the prediction at the LHC energy.

$\sqrt{s}$ (TeV)		σ_{tot} (mb)	ρ
0.55	UA4	62.2 ± 1.5	0.135 ± 0.015
	CDF	61.3 ± 0.9	
	Fit	61.8 ± 0.7	0.138 ± 0.010
0.90	UA5	65.3 ± 1.7	
	Fit	67.5 ± 1.3	
1.8	E710	72.8 ± 3.1	0.140 ± 0.069
	CDF	80.0 ± 2.2	
	Fit	76.5 ± 2.3	0.142 ± 0.015
14	Fit	109 ± 8	0.134 ± 0.018

Table 1. The high-energy data on σ_{tot} and ρ from ref.[6,7,8,9,10] are listed together with the results of the dispersion relations fit of ref.[5].

The experimental results at $\sqrt{s}$=0.55 TeV are well reproduced by the best fit. At $\sqrt{s} = 1.8$ TeV, the fit predicts a value of the total cross section which lies in between the two measurements[8, 9] reported from Fermilab. The result of E710 seems to favour a $\log s$ increase while the result of CDF favours the $(\log s)^2$ dependence. Cosmic ray data[11] have large uncertainties but are consistent with the extrapolation of ref.[5].

In spite of the large error on the parameter γ as derived from the best fit, this dispersion relations analysis clearly favours the $(\log s)^2$ dependence with respect to the linear rise as $\log s$. This behaviour has been often referred to as a "qualitative" saturation of the Froissart-Martin [12] bound in the sense that it corresponds to the maximum rate of rise with energy which is allowed by analyticity and unitarity, while numerically actual data lie much below the bound itself.

At $\sqrt{s} = 14$ TeV the fit predicts $\sigma_{tot} = 109 \pm 8$ mb while extrapolating as $\log s$, one would obtain $\sigma_{tot} \simeq 95$ mb, i.e. about 15 mb less than the $(\log s)^2$ extrapolation. The measurement of TOTEM will have accuracy of about 1 mb, clearly sufficient to discriminate between the two possibilities.

The total cross section results in the high-energy region are also shown on an expanded scale in Fig.3 together with the prediction of the "impact picture" by Bourrely, Soffer and Wu[13]. The prediction of the Regge model by Donnachie and Landshoff[14] gives results which are numerically quite similar.

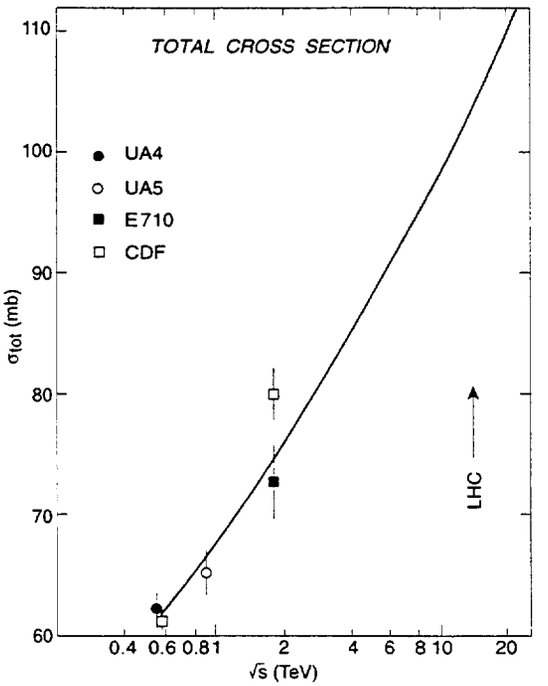

Figure 3: Results on the $\bar{p}p$ total cross section at the highest energies are shown together with the predictions of the impact picture model of ref.[13].

2.2 The Real Part of the Amplitude at t$\simeq$0

In hadron-hadron scattering the real part of the amplitude in the forward direction provides information on the energy dependence of the total cross section. The measurement of the real part complements in an obvious way the measurement of the total cross section, which by virtue of the optical theorem, is just proportional to the imaginary part of the forward amplitude.

General properties of the amplitude as analyticity, unitarity, crossing symmetry and polynomial boundedness imply a correlation between real part and total cross section, as discussed by Khuri and Kinoshita[15]. In the energy region where the total cross section is first decreasing and then rising, the parameter ρ, defined as the ratio of the real to the imaginary part of the forward amplitude, $\rho = ReF(0)/ImF(0)$, has initially a negative value but rises with energy becoming positive. If asymptotically the total cross section saturates the Froissart-Martin bound[12], i.e. if $\sigma_{tot} \sim (\log s)^2$, then ρ will reach a broad maximum and then slowly decrease toward zero as $\pi/\log s$. The broad maximum is expected in the c.m.s. energy region around 1 TeV.

A rise of the total cross section with energy which is less fast than that allowed by this bound implies that ρ will approach zero more rapidly.

In practice the analysis of the data on σ_{tot} and ρ is performed with the standard dispersion relations, however, the information provided by the knowledge of the real part can be qualitatively understood from the approximate expression known as

"derivative dispersion relation".

$$\rho \simeq \frac{\pi}{2\sigma_{tot}} \frac{d\sigma_{tot}}{d \log s}$$

The correlation between σ_{tot} and ρ has been exploited to predict the behaviour of the total cross section at energies higher than those at which the measurements were actually performed. Predictions on the high-energy behaviour of σ_{tot} were made at the ISR[16, 17] and at the SPS Collider[5]. A compilation of data and predictions on the parameter ρ are shown in Fig.4.

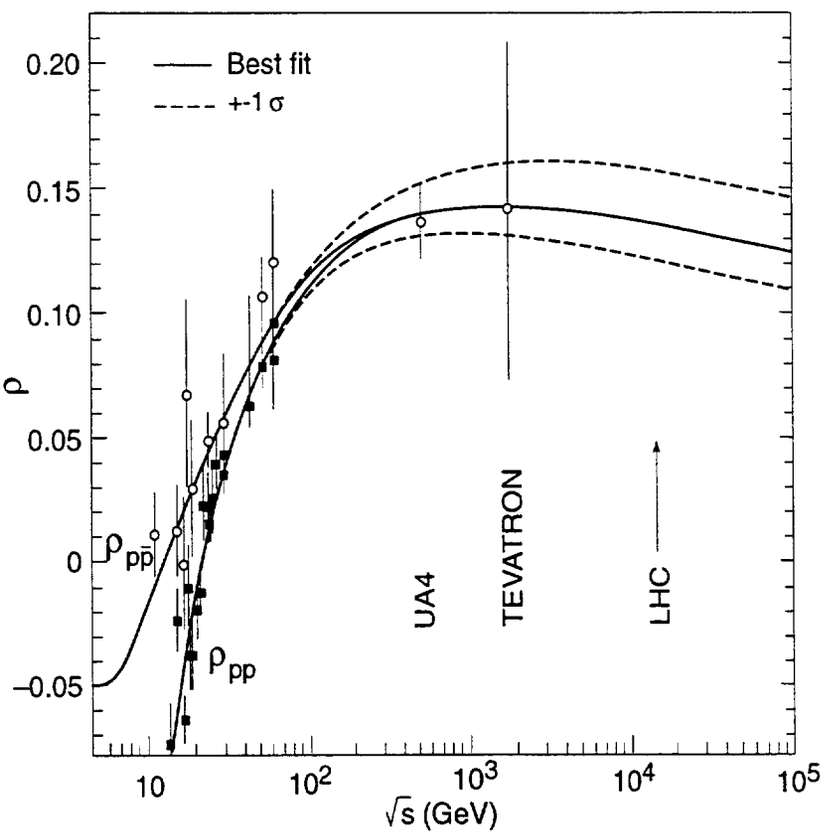

Figure 4: The ratio ρ of the real to the imaginary part of the forward amplitude for $\bar{p}p$ and pp scattering. The prediction of the dispersion relations fit of ref.[5] (solid line) is shown together with the region of uncertainty delimited by the dashed lines.

An unconventional and exciting possibility was discussed recently by Khuri [18]. The presence of a fundamental length R would imply a breakdown of Quantum Field Theory and as a consequence also of the dispersion relations. At present from QED and the results on the muon magnetic moment one may set a limit and rule out the existence of a fundamental length R such that $R^{-1} > 1$ TeV. The model calculation of ref.[18] shows that, if $R^{-1} \simeq 10 - 15$ TeV, the actual value of ρ at the LHC might differ substantially from that calculated with the standard

dispersion relations. Therefore the effect, if present, could well be detected by future experiments.

The measurement of the real part of the amplitude near the forward direction requires the study of elastic scattering in the region of the Coulomb interference. The value of the momentum transfer t_0 where the Coulomb and the strong interaction amplitudes are equal in magnitude is given by

$$|t_0| \simeq \frac{8\pi\alpha}{\sigma_{tot}}$$

Because of the rise of σ_{tot} with energy, the value of t_0 becomes smaller at higher energy and therefore the measurement is more difficult. At the LHC one expects $|t_0| \simeq 7{*}10^{-4}$ GeV^2 corresponding to an angle of only 4 μrad. From the experimental point of view, to find a way to detect events at such small scattering angles is a very serious challenge. A suitable technical solution has not been found yet but it is being actively studied.

2.3 Elastic Scattering

A quantity which is quite important for the understanding of the mechanism of high-energy collisions is the ratio σ_{el}/σ_{tot}. Data on this ratio for $\bar{p}p$ are plotted as a function of energy in Fig.5.

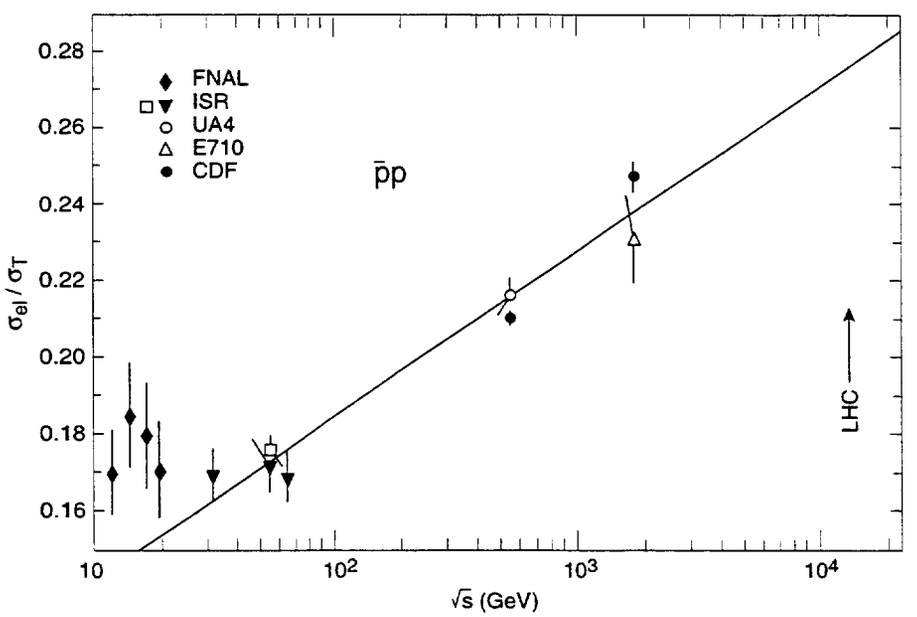

Figure 5: The ratio of the elastic to the total cross section for $\bar{p}p$ interactions as a function of energy. The line is a linear extrapolation to guide the eye.

The Tevatron data confirm the trend already observed at the SPS Collider that the ratio σ_{el}/σ_{tot} increases with energy.

This observation implies that the effective "opacity" of the two colliding particles increases, although slowly, with energy and puts important constraints on the models of high-energy scattering. In fact the accurate determination of this ratio allowed to discriminate between different models. For example the concept of "geometrical scaling" which was very fashionable at the time of the ISR had to be abandoned after the discovery that the ratio σ_{el}/σ_{tot} is increasing in the energy range of the SPS and Fermilab Colliders.

Among existing models of high-energy collisions, this behaviour is most naturally explained in the "impact picture" of Cheng and Wu [19]. They actually predicted that at very high energy the effective radius of interaction of the two colliding hadrons would increase as $\log s$ and that the "opacity" would also increase. This leads to the expectation that asymptotically $\sigma_{tot} \sim (\log s)^2$ and $\sigma_{el}/\sigma_{tot} \to 1/2$.

The measurement of the ratio σ_{el}/σ_{tot} can be made with quite high precision because it essentially corresponds to a ratio of counting rates and therefore some systematic errors disappear. TOTEM plans to measure this ratio at the 1% level.

2.3.1 The forward peak

Near the forward direction ($|t| < 0.1$ GeV^2) the differential cross section is well described by the simple exponential $e^{-B|t|}$. As shown in Fig.6, the high-energy data are consistent with a $\log s$ rise of $B(s)$. This is expected in the classical Regge model which predicts a forward slope of the form $B(s) = B_0 + 2\alpha' \log s$. Numerically the effective slope of the Pomeron trajectory turns out to be $\alpha' \simeq 0.25$ GeV^{-2}.

On the other hand the overall forward peak for $|t| < 0.5$ GeV^2 in general does not show the simple exponential shape $e^{-B|t|}$. In the energy range of the ISR[20] and SPS Collider[21] the shape is concave, the value of the local slope at $t \simeq 0$ being larger by 1.5 - 2 units of GeV^{-2} with respect to the local slope at $|t| \simeq 0.2$ GeV^2. At the Tevatron, however, the curvature seems to have disappeared and the shape of the t-distribution can be described by a single exponential[22]. A compilation of the local slope parameter $B(t)$ as a function of t for different energies is shown in Fig.7.

The change of shape with energy of the forward peak is naturally explained by the impact picture model[13, 19]. At the LHC, this model predicts a reversal of the sign of the curvature, i.e. a convex shape.

The appearence at high energy of a structure or small oscillations superimposed on the simple exponential behaviour of the forward peak has also been discussed[23]. It is not clear whether some indications of this effect are already present in existing data.

In addition, on the basis of general considerations it was shown that the real part of the amplitude is expected to change sign in the low momentum transfer region of the diffraction peak[24].

At LHC there will be the possibility to accumulate high statistics in a short running time and therefore small structures of the forward peak could be easily observed experimentally.

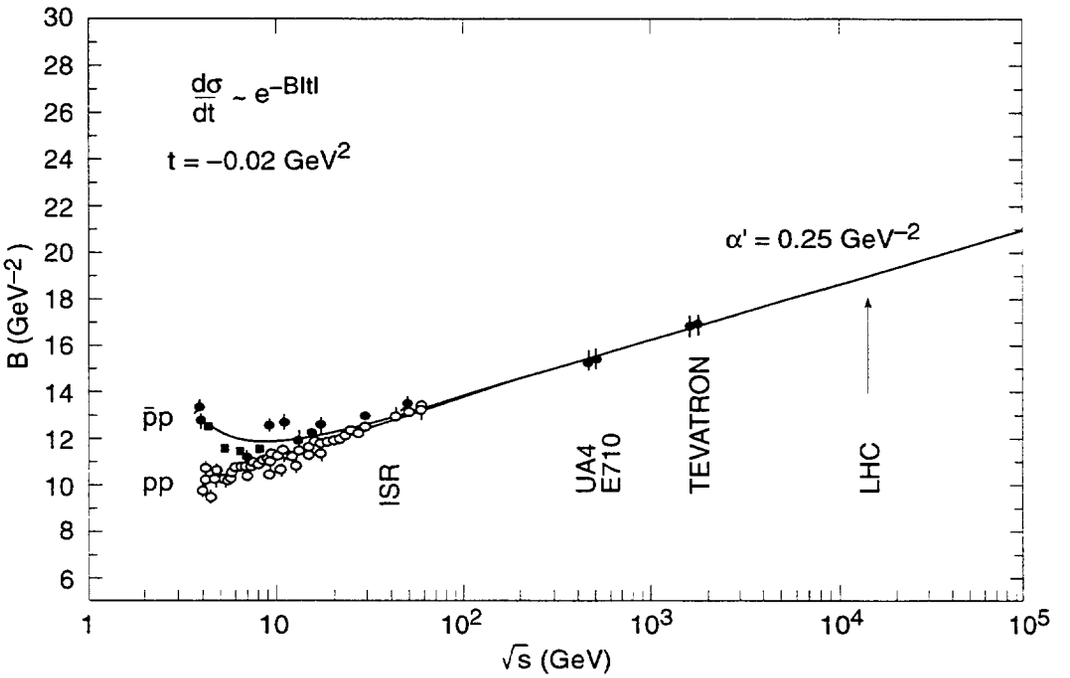

Figure 6: The forward slope parameter B for $\bar{p}p$ and pp elastic scattering. The solid line refers to the Pomeron trajectory of the Regge model.

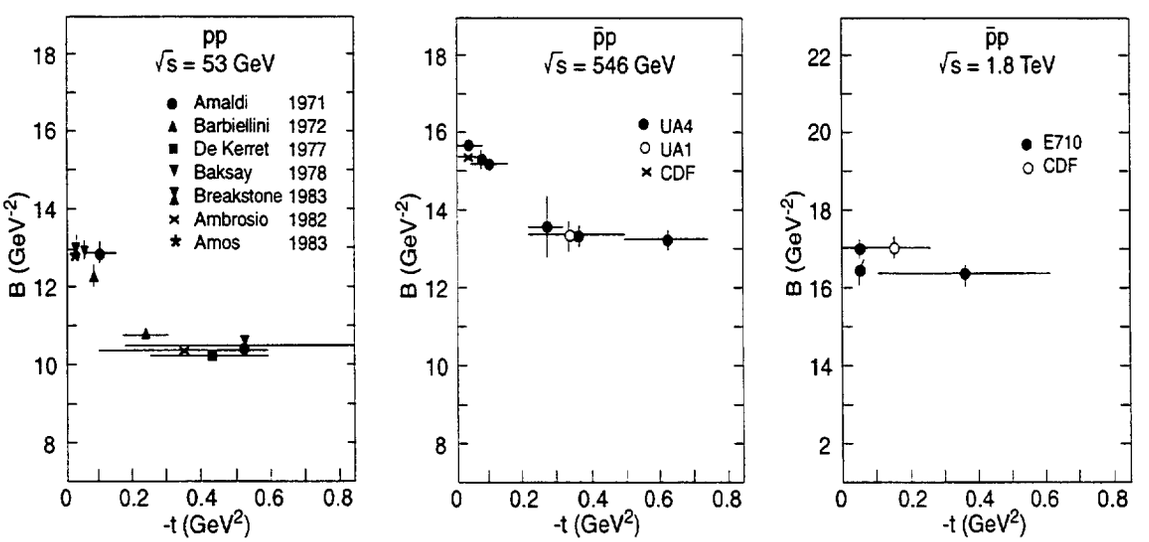

Figure 7: The local slope parameter B(t) is plotted as a function of t for pp and $\bar{p}p$ scattering at different energies

2.3.2 The large momentum transfer region

Of great interest is the large momentum transfer region where at present energies a diffraction-like structure is observed which is followed by a smooth behaviour. The pp and $\bar{p}p$ data differ considerably in the region of the structure because pp scattering shows a pronounced dip[25] while $\bar{p}p$ shows no dip but only a shoulder [26, 27]

This effect is explained by the model of Donnachie and Landshoff [28] as due to the presence of the three-gluon exchange mechanism. The amplitude of this process has different sign for pp and $\bar{p}p$ scattering. Its interference with the main amplitude which describes the diffraction peak is destructive in pp scattering, thus producing a dip, but, on the contrary, is constructive for $\bar{p}p$ giving rise only to a break. We then expect at LHC a dip and not a break.

The cross section of the three-gluon exchange diagram [28] in the limit of large t and very large s, decreases as the eighth power of t.

$$\frac{d\sigma}{dt} = C\frac{1}{t^8}$$

The data on pp scattering at large momentum transfer which are presently available indeed follow this power law for $\mid t \mid \geq 3$ GeV^2 as shown in Fig.8. According to this model, if the three-gluon exchange is the dominant mechanism at large momentum transfer also at higher energies, we expect the t-distribution to be smooth at LHC, without structure.

In addition the model of ref.[28] predicts that $d\sigma/dt$ for fixed and large values of t is energy independent. It should be noted, however, that the possibility of such behaviour was questioned on general grounds by Gribov[29]. The very large energy span from the ISR up to LHC allows a significant study of this point to be made.

There are other predictions which are very different from that of the three-gluon exchange model. As an example we show in Fig.9 the results of two different models, the impact picture[13, 30] and the Regge model of Desgrolard et al.[31]. Both these models are able to reproduce the data at present energies rather well. At higher energy they predict the emergence of a diffraction pattern with several dips in contrast with the three-gluon exchange model.

The difference between the prediction of ref.[28] and those of ref.[30,31] reflects a basic question on the nature of the elastic scattering of hadrons. The question is whether scattering at large momentum transfer results from a single elementary process or is dominated by a complicated interplay of various amplitudes corresponding to higher order of multiple scattering, i.e. of multiple elementary processes at low momentum transfer.

The large design luminosity of the LHC allows elastic scattering to be measured up to large values of the momentum transfer, i.e. in the range 10 - 15 GeV^2. The question of whether pp scattering at very large energy and large momentum transfer has a smooth behaviour or a diffraction-like structure will be resolved experimentally.

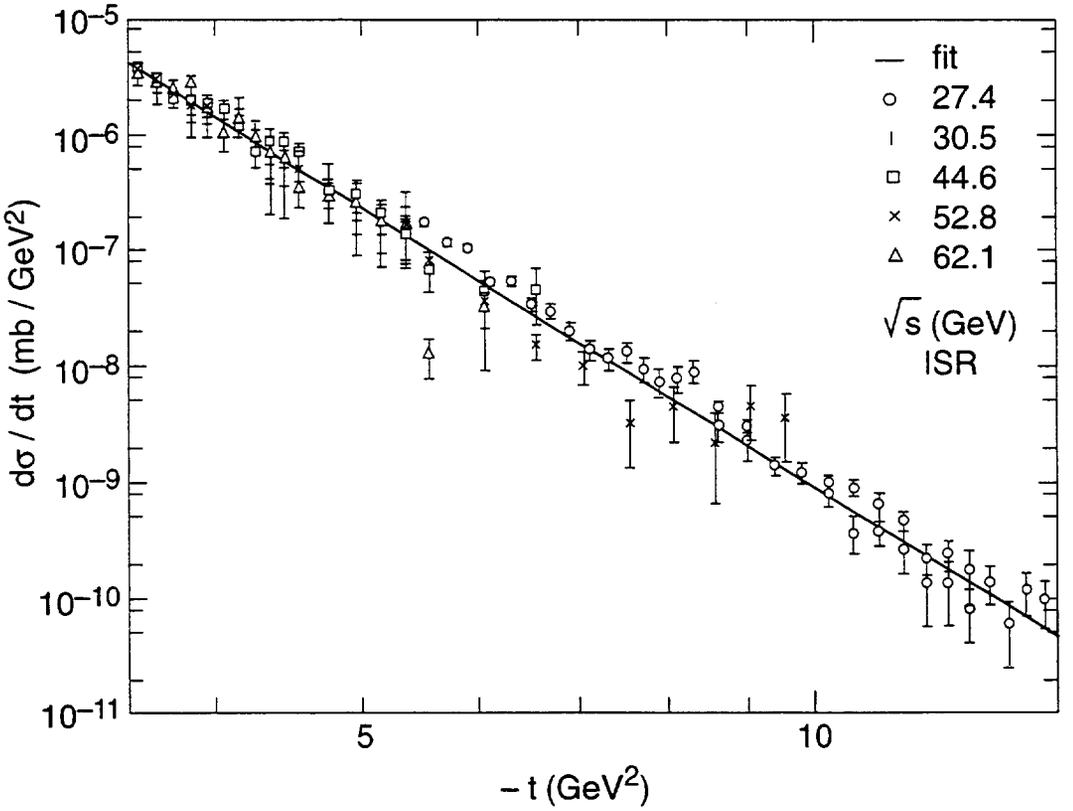

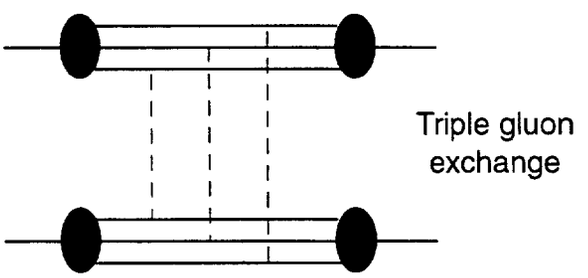

Figure 8: The data on high-energy pp elastic scattering for $|t| \geq 3$ GeV^2 are compared to the prediction of the three-gluon exchange model. The straight line represents the $1/t^8$ behaviour.

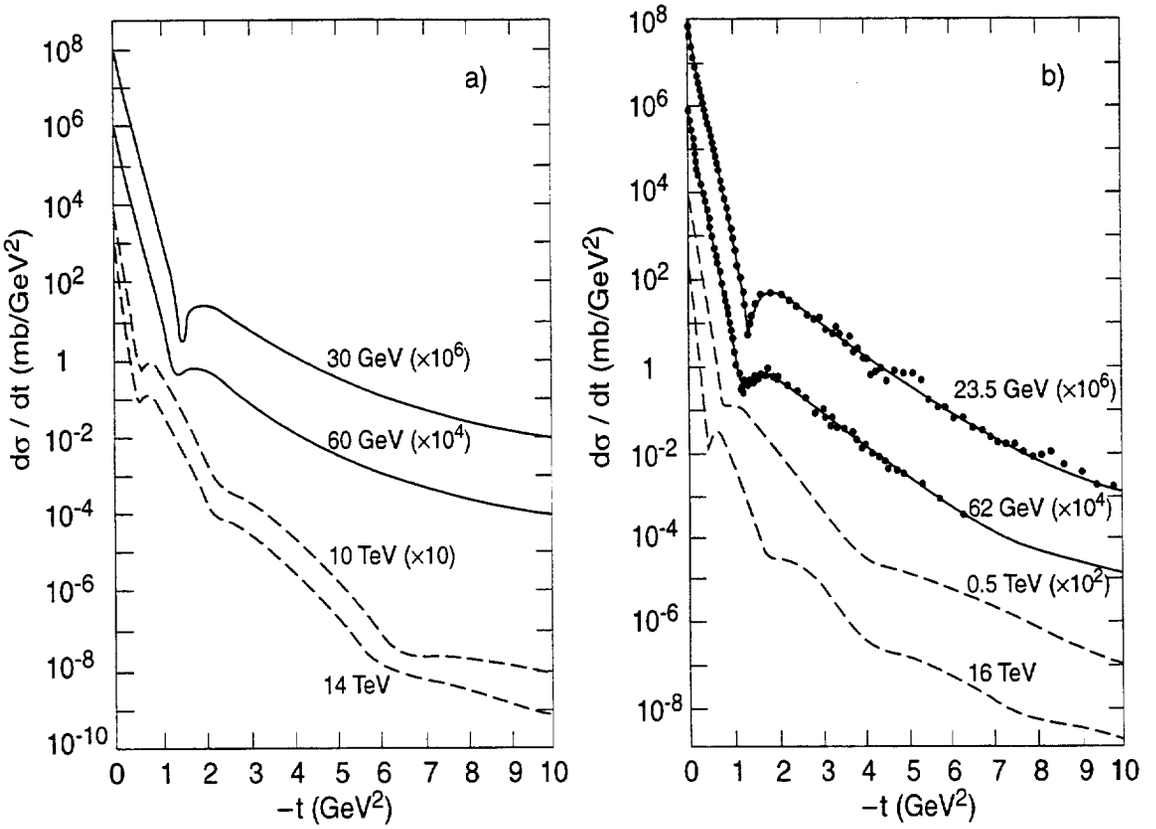

Figure 9: The predictions of two models on pp elastic scattering at high energy: a) ref.[13,30] and b) ref.[31]

2.4 Diffraction Dissociation

The process of diffraction dissociation is closely related to elastic scattering. Single diffraction dissociation may be regarded as a two-body reaction

$$p + p \to p + X$$

where one of the colliding protons is excited to a system X which then decays in a number of stable particles. To be diffractively produced, the system X must have the same intrinsic quantum numbers as the incoming proton while spin and parity may be different because some orbital angular momentum can be transferred to X in the collision.

In a high-energy collision, the mass M of the system X may take quite large values with a limitation which is imposed by the coherence condition as was first remarked by Good and Walker[32]. If p_0 is the beam momentum and p the momentum of the final state proton, the mass M is given by $M^2 = (1 - x)\, s$ where $x = p/p_0$. The coherence condition implies $M^2/s \leq 0.15$ which can be taken as a kind of upper limit. High-energy data indeed provide clear evidence for diffractive production up to $M^2/s \sim 0.05$.

At present energies the integrated cross section of single diffraction dissociation σ_{SD} is a sizeable fraction of the total cross section.

The energy dependence of the ratio of the single diffraction to the total cross section is shown in Fig.10 where it is compared to the ratio of the elastic to the

total cross section. The ISR data on σ_{SD} are from CHLM[33], the SPS Collider data from UA4[34] and the Tevatron data from CDF[35]. The data indicate that

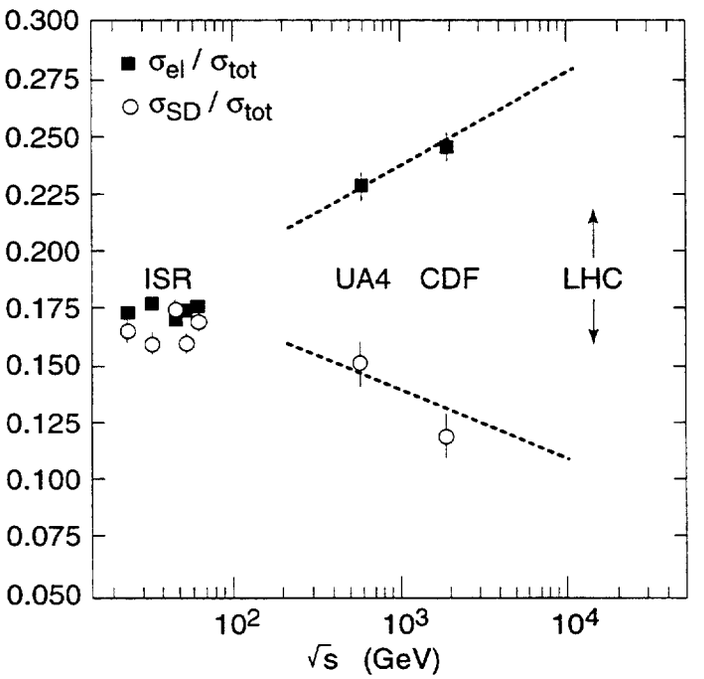

Figure 10: The ratio of the elastic to the total cross section σ_{el}/σ_{tot} , and the ratio of the single diffraction dissociation to the total cross section σ_{SD}/σ_{tot}, are shown as a function of energy. The lines are linear extrapolations to guide the eye.

the probability of diffraction dissociation as compared to the overall probability of interaction decreases with energy. However, in order to obtain an accurate value of the total cross section at LHC, one has to measure σ_{SD} at a reasonable level of precision.

In addition we believe that a measurement of the ratio σ_{SD}/σ_{tot} at LHC is important on its own for a better understanding of the mechanism of hadronic collisions at very high energy.

An important feature about diffraction dissociation to be investigated is the mass dependence of the double differential cross section $\frac{d^2\sigma}{dtdM^2}$. The data from the ISR[33] and the SPS Collider[36], shown in Fig.11 for -t = 0.5 GeV^2, indicate that the mass spectrum has a $1/M^2$ behaviour in agreement with the classical prediction of triple Pomeron exchange.

It is clear that the LHC with its very large c.m.s. energy opens new possibilities because systems with very large mass can be excited by diffraction. In fact at LHC when $M^2 \sim 0.05\ s$, the mass M is as large as 3 TeV.

We are also planning to measure the production of π^0 in the near forward direction. In addition to being a natural complement to the detection of charged particles, this allows studying *scaling in the fragmentation region* at rapidities very close to

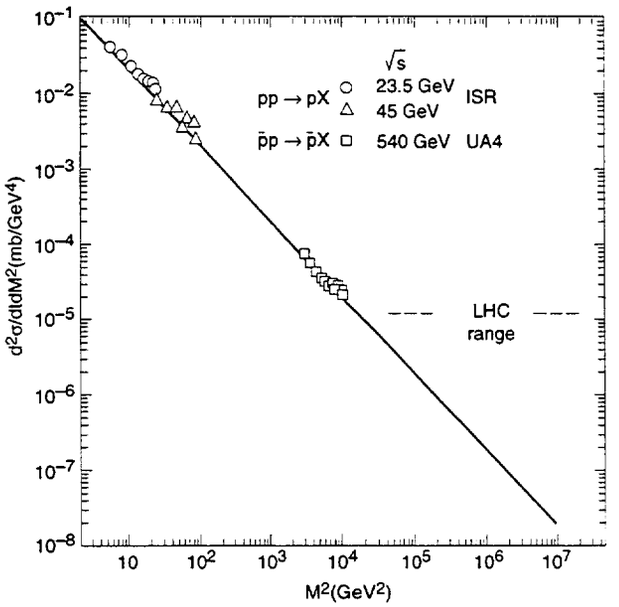

Figure 11: The observed mass spectrum of the diffractively excited system.

the beam rapidity and it is of special interest in connection with the interpretation of very high-energy cosmic ray interactions.

3 The Experimental Method

3.1 Measurement of Elastic Scattering

The measurement of elastic scattering at a high energy hadron collider requires observation of particles at very small angles (at the LHC, typical angles are a small fraction of a *mrad*). In practice this is achieved by placing the detectors into special units mounted on the vacuum chamber of the accelerator, which have become known as "Roman pots" and were first used at the CERN ISR.

In its retracted position the "Roman pot" leaves the full aperture of the vacuum chamber free for the beam, as required at the injection stage when the beam is wide. Once the final energy is attained and the circulating beams are stable, the "Roman pot" is moved toward the machine axis by compressing the bellow, until the inner edge of the detector reaches a distance of the order of one *millimeter* from the beam. There is no interference with the machine vacuum.

Hadron colliders are usually operated at high luminosity for the search of rare events. To obtain high luminosity, the transverse size of the beam at the crossing point is reduced by the focusing action of quadrupoles. As a consequence the angular divergence of the beams is correspondingly increased so that a large fraction of the scattered particles remain inside the acceptance of the machine itself and are not accessible to detection.

To measure elastic scattering, the opposite scheme is actually required. The beam size at the crossing point is made relatively large while the beam divergence becomes very small. Nearly parallel beams are normally used. This implies that the β-function at the crossing point has to be large. The corresponding loss of luminosity is not a problem because the differential cross section of elastic scattering is large at small t.

The best arrangement[37] is obtained by placing the detectors at a distance from the crossing point equal to one quarter of the period of the betatron oscillations. In that case an optics with parallel-to-point focusing from the crossing point to the detectors is achieved. This has the very convenient property that measuring the particle position at the detector allows the scattering angle to be reconstructed in a straightforward way.

The method is basically the same as the classical technique of measuring the direction of light rays by means of an optical system with a screen placed on the focal plane.

3.1.1 General considerations

We now proceed with a discussion of the experimental method for measuring elastic scattering in a quite general way, independently of the specific realization of the insertion, detectors and vacuum chambers.

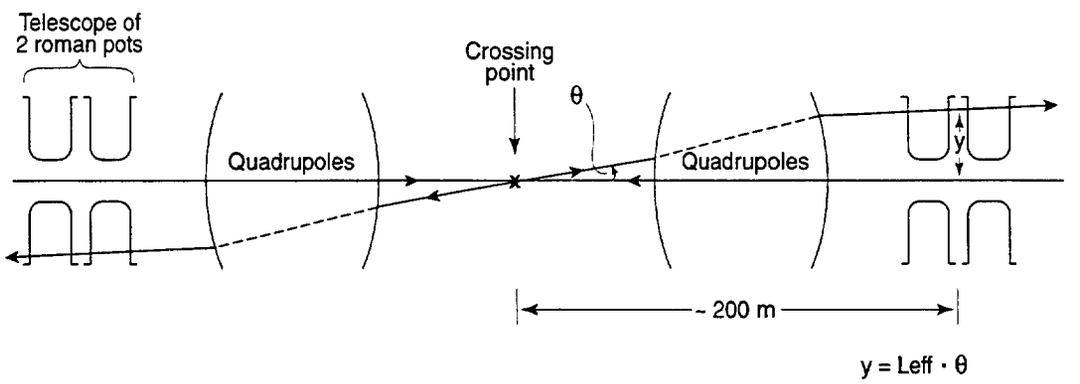

Figure 12: Sketch of the layout of the elastic scattering experiment - side view. The effective distance L_{eff} is determined by the optics of the insertion.

The typical layout is sketched in Fig.12. The detectors are placed in a long straight section of the accelerator on both sides of the crossing point. Between the detectors and the crossing point there will be magnetic elements of the machine, i.e. dipoles used to bring the two beams together at the crossing and quadrupoles. We assume to measure elastic scattering in the vertical plane because in the vertical plane the beams are usually more stable. On each beam, downstream of the crossing point, there will be a telescope of two Roman pots placed a few meters apart

and therefore able to measure both the position and the direction of the scattered protons.

Let y^* be the vertical coordinate of the collision point and $y_L^{*\prime}$, $y_R^{*\prime}$ the projections on the vertical plane of the angles of the two scattered protons, on the left and right side, respectively. In the ideal case of parallel beams, $y_L^{*\prime}$ and $y_R^{*\prime}$ would be equal to the vertical component of the scattering angle. Displacements and angles of the scattered protons at the detectors are expressed as a function of the displacement and angles at the crossing point by the following equations

$$\begin{pmatrix} y_L \\ y'_L \end{pmatrix} = \begin{pmatrix} M_{11}^L & M_{12}^L \\ M_{21}^L & M_{22}^L \end{pmatrix} \begin{pmatrix} y^* \\ y_L^{*\prime} \end{pmatrix} \tag{1}$$

$$\begin{pmatrix} y_R \\ y'_R \end{pmatrix} = \begin{pmatrix} M_{11}^R & M_{12}^R \\ M_{21}^R & M_{22}^R \end{pmatrix} \begin{pmatrix} y^* \\ y_R^{*\prime} \end{pmatrix} \tag{2}$$

where $\|M^L\|$ and $\|M^R\|$ are the transfer matrices from the crossing to the detectors on the left and right side, respectively.

In principle the measurement of the positions and angles y_L, y_R, y'_L and y'_R at the detectors allows the determination of the three unknown quantities y^*, $y_L^{*\prime}$ and $y_R^{*\prime}$ referring to the crossing. However, the direction is not measured accurately enough because the detectors making a telescope cannot be too far apart while they have to be placed far away from the crossing and therefore the lever arm is quite unfavourable. This difficulty, however, can be avoided by using an insertion with optics which is left-right symmetric.

From eqs.[1,2], combining the observed displacements on the left and right arms, one finds

$$\bar{y} = \frac{1}{2}(y_R - y_L) = \frac{1}{2}(M_{11}^R - M_{11}^L)y^* + \frac{1}{2}(M_{12}^R y_R^{*\prime} - M_{12}^L y_L^{*\prime}) \tag{3}$$

For a symmetric optics, which is defined by the relationships

$$M_{11}^L = M_{11}^R \ , \ M_{12}^L = -M_{12}^R \ , \ M_{21}^L = -M_{21}^R \ , \ M_{22}^L = M_{22}^R$$

the term involving the vertical position of the collision point drops out and eq.[3] reduces to:

$$\bar{y} = \frac{1}{2} M_{12}(y_R^{*\prime} + y_L^{*\prime}) \tag{4}$$

where $M_{ij} = M_{ij}^R$.

In the ideal case of parallel beams without any angular spread,

$$y_L^{*\prime} = y_R^{*\prime} = \vartheta_y$$

where ϑ_y is the vertical component of the scattering angle. In practice, the actual angles of the incoming protons will add to the scattering angle ϑ_y thus making $y_L^{*\prime}$ and $y_R^{*\prime}$ somewhat different. In any case, however, the best estimate of ϑ_y will still be obtained from eq.[4]:

$$\vartheta_y = \frac{1}{2}\frac{y_R - y_L}{M_{12}}$$

From eqs.[1,2] we get the following equations

$$y_R^{*\prime} = \frac{y_R - M_{11} y^*}{M_{12}} \quad , \quad y_L^{*\prime} = -\frac{y_L - M_{11} y^*}{M_{12}} \tag{5}$$

A crucial requirement for the present experiment is to reach the smallest possible value of the scattering angle. From eq.[5] it is clear that the best strategy is to design the optics of the insertion with the conditions

- $M_{11} = 0$
- M_{12} as large as possible

The determinant of the transfer matrices being equal to one, the condition $M_{11} = 0$ implies

$$M_{21} = -\frac{1}{M_{12}}$$

while no condition is imposed on the element M_{22}.

The condition $M_{11} = 0$ defines the optics as a *parallel to point focusing* from the crossing to the detectors. Particles scattered in the same direction are brought together to the same point on the detector independently of the position of the collision point. This is clearly the best possible arrangement because the measurement of the angle, which is the physically relevant quantity, becomes decoupled from the measurement of the position of the collision point. In this configuration the beam size at the crossing point becomes irrelevant and the displacement y at the detector is uniquely determined by the scattering angle.

In this special case of a *parallel to point focusing* optics, the matrix element M_{12} represents the effective distance of the detectors from the crossing point and we have the simple relations

$$y_L = -L_{eff}\, y_L^{*\prime} \quad , \quad y_R = L_{eff}\, y_R^{*\prime} \tag{6}$$

The vertical, and main component of the scattering angle is given by

$$\vartheta_y = \frac{1}{2} \frac{y_R - y_L}{L_{eff}} \tag{7}$$

For ideal, exactly parallel beams, all particles emitted at the same angle at the crossing will be focused to a point onto the detector. In practice, however, each beam will have an angular spread (say $\Delta\vartheta_y^{(beam)}$ in the vertical plane) due to betatron oscillations. Therefore the beam spot on the detector will be given by

$$\Delta y^{(spot)} = L_{eff}\, \Delta\vartheta_y^{(beam)} \tag{8}$$

The actual uncertainty on the vertical component of the scattering angle $\Delta\vartheta_y$ results from the quadratic combination of the detector resolution $\Delta y^{(det)}$ and the intrinsic angular spread of the beams.

$$\Delta\vartheta_y = \frac{1}{\sqrt{2}} \left(\frac{\Delta y^{(det)}}{L_{eff}} \bigoplus \Delta\vartheta_y^{(beam)} \right) \tag{9}$$

With detectors of infinitely good precision the error on ϑ_y would be due just to the intrinsic angular spread of the beams. In practice one should choose detectors with spatial resolution somewhat smaller than the size of the spot at the detector, as given by eq.(8).

The coordinate of the collision point is obtained from the equations

$$y^* = M_{22} y_R - M_{12} y'_R \quad , \quad y^* = M_{22} y_L + M_{12} y'_L$$

using both left and right arms. As a first approximation, one may neglect the angular spread of the beams. In that case $y_R \approx y_L$ and therefore

$$y^* \approx \frac{1}{2}(y'_L - y'_R) M_{12} = y^* \approx \frac{1}{2}(y'_L - y'_R) L_{eff} \tag{10}$$

The error on the position of the collision point will be

$$\Delta y^* \approx \frac{1}{\sqrt{2}} L_{eff} \Delta y'^{(det)} \tag{11}$$

where $\Delta y'^{(det)}$ is the uncertainty on the vertical slope of the trajectory as measured by the Roman pot telescope. The presence of un unfavourable lever arm will make the determination of the position of the collision point not very accurate. It will not be possible to reconstruct the actual space distribution of the collision points. It is possible, however, to keep the error Δy^* substantially smaller than the transverse size of the vacuum chamber in order to be able to disentangle beam-beam events from beam-wall background.

In the horizontal plane, there is no special additional requirement, once the basic condition of a left-right symmetric optics is implemented. It is very desirable, however, to have the matrix element $M_{12}(hor)$ similar in magnitude to $M_{12}(vert)$.

The momentum transfer resolution will be given by

$$\Delta t = 2p\sqrt{|t|}\Delta\vartheta \tag{12}$$

where $\Delta\vartheta$ is the error on the scattering angle.

3.1.2 Requirements on the insertion

On the basis of the general discussion given in the previous section, we may now define the requirements on the machine optics in the long straight section. We don't consider here the possibility of placing the "Roman pots" behind the dipoles of the machine arcs. This option will generally reduce the angular acceptance of the detectors and possibly interfere with the cryogenic system of the machine. It will become immediately clear that the measurement of low-t elastic scattering is feasible only in a *special insertion with high* β^*.

Using standard notations of accelerator physics and referring again to the projection on the vertical plane, we write the displacement y at the detector as a function of the displacement y^* at the crossing point and of the scattering angle ϑ as

$$y = \sqrt{\beta_d/\beta^*}(\cos\Delta\psi + \alpha^* \sin\Delta\psi) y^* + (\sqrt{\beta^*\beta_d}\sin\Delta\psi)\vartheta \tag{13}$$

where β^* and β_d are the values of the betatron function (in the vertical plane) at the crossing point and at the detector respectively. The phase advance of the betatron oscillations from the crossing to the detector is $\Delta\psi = \int ds/\beta(s)$ and $\alpha^* = -\frac{1}{2}(d\beta^*/ds)$. The beam size σ_y and the beam angular divergence σ_ϑ are written in terms of the emittance ϵ (defined at the one r.m.s. value) as $\sigma_y = \sqrt{\epsilon\beta}$ and $\sigma_\vartheta = \sqrt{\epsilon/\beta}$. The quantity $\sqrt{\beta^*\beta_d}\sin\Delta\psi$ represents the effective distance L_{eff} of the elastic detectors from the crossing point.

Insertions are usually designed with the β-function symmetric around the crossing point, i.e., α^*=0. This is not, however, a necessary requirement and it is possible that by releasing this condition one might gain some additional flexibility which could be useful for an optimized design of the insertion.

The best configuration for elastic scattering, as already discussed, corresponds to the optics with *parallel-to-point* focusing from the crossing to the detectors. This is achieved when *the elastic detectors are placed at the position where the phase advance is* $\Delta\psi = \pi/2$.

$$y = L_{eff}\,\vartheta \quad , \quad L_{eff} = \sqrt{\beta^*\beta_d}$$

The minimum distance of approach of the inner edge of the detectors to the beam axis, y_d, is proportional to the r.m.s. value of the beam size at the detector position σ_y. We may write

$$y_d = K\sigma_y = K\sqrt{\epsilon\beta_d} \tag{14}$$

At the SPS Collider it was empirically found by the experiment UA4 that the parameter K had numerical values between 15 and 20, depending on the machine conditions. In the same experiment a space of about 1 mm between the inner edge of the detector and the edge of the "Roman pot" was lost for reasons of mechanical construction. We assume that with a new design this dead space will be reduced and be negligible at LHC.

In the following considerations we assume that space will be available in the straight section in the region where $\Delta\psi = \pi/2$ to place the Roman pots. For the protons which hit the detector just on its inner edge, the scattering angle and the corresponding momentum transfer will be

$$\vartheta_d = \frac{K\sqrt{\epsilon}}{\sqrt{\beta^*}} \quad , \quad |t_d| = K^2p^2\frac{\epsilon}{\beta^*} \tag{15}$$

We notice that the angle ϑ_d corresponds to a zero value of the acceptance which reaches useful values for

$$\vartheta_{min} \approx \sqrt{2}\,\vartheta_d \quad , \quad |t_{min}| \approx 2\,|t_d| \tag{16}$$

For a given emittance ϵ, *small values of the momentum transfer are reached for large* β^* *and small* K.

The parameter K may be controlled by the system of collimators which will protect the detectors from being hit by particles of the beam halo. In the present design of the LHC a sophisticated system of primary and secondary collimators is

foreseen[38]. The collimators will be set at a distance from the beam axis equal to 6 σ_{beam} (where σ_{beam} is the r.m.s. beam radius). In these conditions the maximum excursion of the secondary halo should not exceed 10 σ_{beam} and the mechanical aperture around the LHC ring was designed accordingly. Therefore for the design of the present experiment it appears safe to assume $K = 15$ while even smaller values, $K = 10 - 12$ are most likely realistic. A more detailed discussion on this point will be presented in Section 4.5.1.

Using for the beam emittance the value $\epsilon = 5 * 10^{-10}$ m at the nominal beam momentum, $p = 7$ TeV, we can make the following estimates for two different options.

1) *Extrapolation of the elastic rate to the optical point for the measurement of* σ_{tot}. At low t, $dN/dt \sim e^{-B|t|}$ and the slope parameter B is expected at LHC to be $B \approx 20$ GeV^{-2}. The extrapolation to the optical point will be of about 20% for $|t_{min}| \simeq 10^{-2}$ GeV^2 (corresponding to $\vartheta_{min} \simeq 14\ \mu rad$).

$$For\ |t_{min}| \simeq 10^{-2}\ GeV^2,\ eq.(15,16)\ give\ \beta^* \simeq 1100\ m.$$

2) *Measurement of Coulomb scattering.* The minimum value of t should be $|t_{min}| \simeq 5 * 10^{-4}$ GeV^2 (corresponding to $\vartheta_{min} \simeq 3\ \mu rad$).

$$For\ |t_{min}| \simeq 5 * 10^{-4}\ GeV^2,\ eq.(15,16)\ give\ \beta^* \simeq 20000\ m\ .$$

An additional requirement comes from the fact that the actual distance y_d of the inner edge of the detectors from the machine axis should not be too small, in order to avoid problems from possible beam instabilities. A too small value of y_d would also put unrealistic constraints on the mechanical construction of the Roman pots and of the detectors. We tentatively assume a minimum acceptable value for y_d of 1.5 mm. This requirement can be written as

$$L_{eff}\ \vartheta_d \geq y_d(min) = 1.5\ mm \tag{17}$$

and implies that, once the minimum angle is fixed by considerations of physics, the effective distance $L_{eff} = \sqrt{\beta^* \beta_d}$ must not be less than a certain value. For the two options mentioned above, eq.(17) gives

1) $L_{eff} \geq 150$ m

2) $L_{eff} \geq 650$ m

For a given value of β^*, already fixed by the requirement of minimum t, eq.(17) can be translated into the following condition on the value of the β-function at the detectors,

$$\beta_d \geq \frac{y_d^2(min)}{K^2\ \epsilon} \tag{18}$$

Numerically this implies

$$\beta_d \geq 20m$$

In spite of the reduction due to the increased size of the beam at the crossing, the luminosity in the proposed high-β^* insertions will still be so large that for low-t

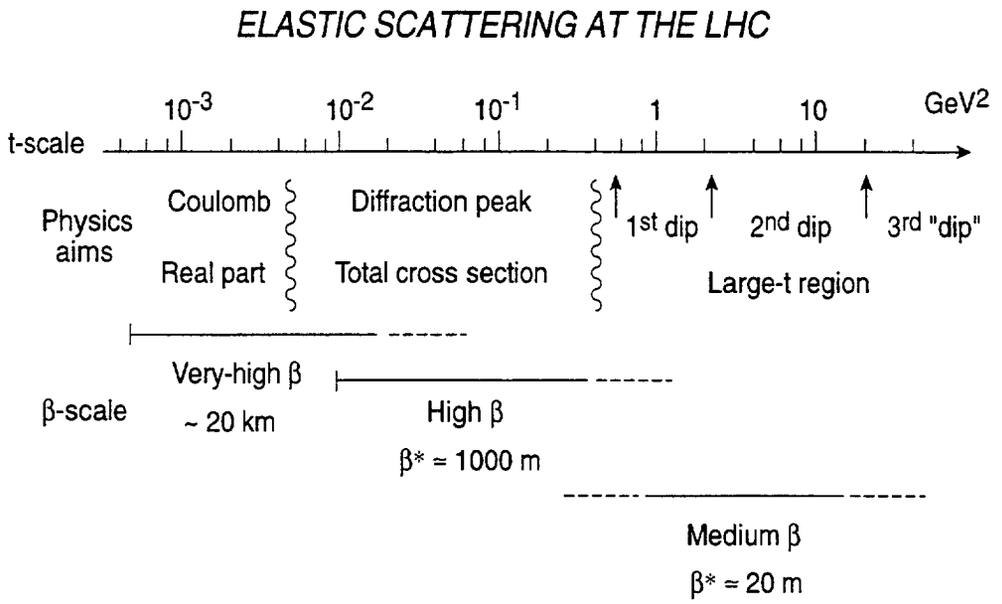

Figure 13: The proposed scheme for a complete study of elastic scattering at LHC. The medium β^* optics is practically the same which is needed by the machine for the injection.

diffractive processes there is a very large margin of safety to ensure a substantial event rate.

The insertion for TOTEM should be designed with a tunable β^* to allow measurement of elastic scattering also in the large momentum transfer region.

On the basis of our previous experience at the SPS Collider, we suggest the scheme of Fig.13 where the insertion is operated at high-β^* for elastic scattering at low-t and at medium-β^* for large-t. We remark that the medium-β^* optics ($\beta^* \sim$ 20 m) does not put any additional constraint on the design of the high-β^* insertion. In fact an optics with β^* of the order of 50 m is needed anyway at the injection.

The options for a design of a tunable β^* insertion at LHC have been recently discussed by A.Verdier[39].

We make a final remark to this Section. We realize that the insertion with the very large β^* needed for Coulomb scattering may be very difficult or even unrealistic to design because of several machine constraints. We believe, however, that it should not be discarded at this early stage as definitely impossible.

3.2 Operational Aspects of the Machine

As already stated in the Introduction, the measurement of the total cross section requires only a very modest luminosity and, due to the peculiarity of the experiment could be done in special dedicated runs at the start of the LHC.

Therefore we propose to operate with a number of bunches n_b^{el} which is reduced

with respect to the maximum number of bunches n_b^{max} foreseen in LHC. The experiment will thereby benefit from several advantages:

(i) a luminosity lower by a factor n_b^{el}/n_b^{max},

(ii) no long range interactions at zero crossing angle,

(iii) trigger and data acquisition are simplified due to long bunch spacing and thereby also lower background.

Example: - $n_b \approx 12 - 36$ i.e. 1-3 bunches per SPS batch
- $\beta_{el}^* \geq 500 - 1500\ m$ vs $0.5\ m$ for high luminosity L.
- $n_p \approx 10^{10}$-10^{11} adjustable to L^{eff} required;

$$L^{eff} = L^{max} \times \frac{\beta_{min}^*}{\beta_{el}^*} \times \frac{n_b^{el}}{n_b^{max}} \times \left(\frac{n_p^{el}}{n_p^{max}}\right)^2 \qquad (19)$$

$$10^{34} \times 10^{-3} \times 10^{-2} \times 10^{-1}$$

Therefore

$$L^{eff} = 10^{-6} \times L^{max} = 10^{28} cm^{-2} s^{-1}$$

Running at L $\sim 10^{28}$ cm^{-2} s^{-1} would allow a yield of $\sim 10^7$ elastic events per day assuming $\sigma_{tot} = 110$ mb (28% elastic) and an overall running efficiency of $\sim 50\%$.

We will consider this value of the luminosity as a reference for the total cross section and low-t elastic scattering when discussing rates and backgrounds.

It should be noted that this operational scheme fits naturally into the normal start-up and machine development program of the LHC[40]. Early physics results may therefore be expected.

3.3 Measurement of the Total Cross Section

The best way to measure the total cross section is by means of the so called "luminosity independent method". In fact if no accurate and reliable measurement of the machine luminosity is available, this will be the only method which is of practical use. The total cross section and the integrated luminosity $\mathcal{L}$ of the machine are related by the equation

$$N_{el} + N_{inel} = \mathcal{L}\ \sigma_{tot}$$

where N_{el} and N_{inel} are the observed numbers of elastic and inelastic interactions respectively. The optical theorem which relates the total cross section to the imaginary part of the forward amplitude leads to the following equation.

$$\left(\frac{dN_{el}}{dt}\right)_{t=0} = \mathcal{L}\left(\frac{d\sigma}{dt}\right)_{t=0} = \mathcal{L}\frac{\sigma_{tot}^2(1+\rho^2)}{16\pi}$$

Combining the two previous equations one may eliminate the machine luminosity and write the total cross section as a function of measurable quantities in the following way.

$$\sigma_{tot} = \frac{16\pi}{(1+\rho^2)} \frac{(dN_{el}/dt)_{t=0}}{N_{el} + N_{inel}}$$

This method is based on the simultaneous detection of elastic scattering at low t and of the number of the inelastic interactions. The parameter ρ is small at high-energy, about $0.1 - 0.2$, so that it does not have to be known with high precision to get an accurate value of σ_{tot}.

The "luminosity independent method" was used at the ISR by the CERN-Pisa-Roma-Stony Brook collaboration, at the SPS Collider by UA4 and at the Fermilab Collider by E710 and CDF.

The elastic scattering t-distribution dN_{el}/dt is measured at small t using the "Roman pot" system and extrapolated to $t = 0$, i.e. to the so called "optical point", assuming the simple exponential dependence $e^{-B|t|}$ which is known to describe the data adequately in the very small t region.

At LHC we expect $B \approx 20\ GeV^{-2}$, as indicated in Fig.6. In order to measure the total cross section, one has to extrapolate the elastic scattering distribution dN_{el}/dt to the optical point (t=0). If we want to extrapolate by not more than 20%, the minimum value of t should be $\mid t_{min} \mid \approx 10^{-2} GeV^2$.

We notice that

$$\frac{dN_{el}}{dt} = \frac{\pi}{p^2} \frac{dN_{el}}{d\Omega}$$

The quantity $dN_{el}/d\Omega$ is obtained from the number of elastic events which is observed as a function of the scattering angle and from geometric measurements. The contribution to the final error on σ_{tot} coming from the uncertainty Δp on the absolute value of the beam momentum is $\frac{\Delta\sigma_{tot}}{\sigma_{tot}} = 2\frac{\Delta p}{p}$.

3.3.1 The inclusive trigger

The total number of inelastic events N_{inel} will be measured by the *forward inelastic detector* which has to fulfill two basic requirements.

- A "fully inclusive" trigger, sometimes called "minimum bias trigger".
- Identification of beam-beam events against background.

At present collider energies, a sizeable fraction of the inelastic events (about 15 %) are of diffractive type, where the recoil proton, scattered at very small angles, remains inside the vacuum pipe while a few particles are emitted in the opposite hemisphere in the angular region known as fragmentation region. Events of this kind will be observed with a "single arm" trigger using the *inelastic detector* which provides the reconstruction of the interaction vertex from the observed charged tracks. In order to reduce the background, the recoil proton can be detected in coincidence by means of the "Roman pots" in the opposite hemisphere.

The angular coverage which is needed for a fully inclusive trigger can be estimated on the basis of previous experience at the SPS collider and at the Tevatron. The experiments UA4[6] at the SPS Collider and CDF[9] at the Tevatron have covered more than 3 pseudorapidity units extending below $\eta_{max} \simeq y_{beam} - 1$. The experiment E710[8] at the Tevatron has covered a somewhat smaller pseudorapidity interval. The fraction ΔN_{inel} of undetected inelastic events was estimated empirically by extrapolation to the full solid angle by UA4 and E710 while it was estimated using the UA5 intermediate cluster Monte Carlo by CDF.

Results from previous experiments are presented in Table 2.

	$\sqrt{s}(TeV)$	y_{beam}	η_{min}	η_{max}	$\Delta\eta$	$y_{beam} - \eta_{max}$	ΔN_{inel}
UA4	0.55	6.4	2.5	5.6	3.1	0.8	$1.0 \pm 0.3\%$
E710	1.8	7.6	5.2	6.5	1.3	1.1	$3.2 \pm 1.6\%$
CDF	1.8	7.6	3.2	6.7	3.5	0.9	$1.3 \pm 0.4\%$

Table 2. The pseudorapidity coverage of the inclusive trigger is listed for previous experiments together with their own estimates of the loss of inelastic events.

A Monte Carlo simulation of the efficiency of the trigger was performed using the standard program PYTHIA[41] with appropriate tuning of the parameter which controls low-p_t production. This simulation seems to be realistic because it reproduces pseudorapidity distributions at present energies reasonably well. The predicted pseudorapidity distribution of charged particles at $\sqrt{s} = 14$ TeV for non-single diffractive events is shown in Fig.14.

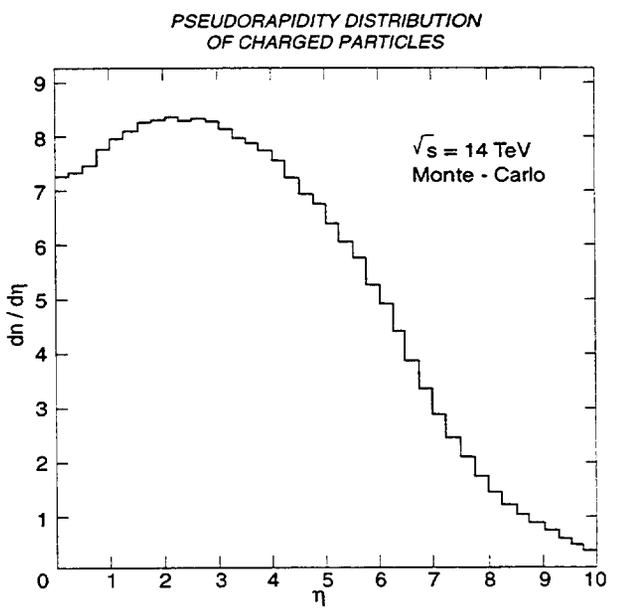

Figure 14: Pseudorapidity distributions of charged particles for non-single diffractive events at the LHC from Monte Carlo simulation.

The results of the simulation for the efficiency of the inclusive trigger used in previous experiments (UA4, E710 and CDF) are presented in Table 3. They agree qualitatively with the estimates made by the experiments themselves, which were shown in Table 2.

	$\sqrt{s}(TeV)$	$\sigma_{SD}/\sigma_{inel}$	Eff_{NSD}	Eff_{SD}	$\text{Eff}_{overall}$	ΔN_{inel}
UA4	0.55	0.18	0.999	0.900	0.981	1.9 %
E710	1.8	0.16	0.975	0.729	0.936	6.4 %
CDF	1.8	0.16	0.999	0.926	0.987	1.3 %

Table 3. Results of the simulation for the loss of inelastic events, ΔN_{inel} in previous experiments. Partial and overall efficiencies for single diffraction and non single diffraction events are given. The value assumed for the ratio of the single diffraction to the overall inelastic cross section is also quoted.

The prediction of the Monte Carlo for the trigger efficiency at $\sqrt{s} = 14$ TeV are shown in Fig. 15 where lines of constant fractional loss on N_{inel} are shown as a function of the lower and upper extremes of the pseudorapidity interval covered by the *inelastic detector.*

These results confirm the simple expectation that in order to keep the loss of inelastic events to the level of 1%, the coverage has to be of at least 3 pseudorapidity units close to the beam rapidity. There is, however, some flexibility in the sense that a given loss can be obtained by choosing different combinations of η_{min} and η_{max}. This implies flexibility in the design of the *forward inelastic detector* which may turn out to be useful to avoid incompatibility with existing equipment placed in the straight section.

In our opinion the results of this simulation, even if not to be taken too quantitavely, should represent a reasonable and useful guide line.

3.4 Measurement of Diffraction Dissociation

The detectors needed to measure the total cross section and elastic scattering will be used also to measure the basic properties of the single diffraction dissociation.

$$p + p \rightarrow p + X$$

The proton scattered quasi-elastically which recoils against the system X will be detected by the telescope of Roman pots of one arm in coincidence with the inelastic detector of the opposite hemisphere.

In the high-β^* insertion (see Section 4.1) there will be strong dipoles for the separation of the two beams and various quadrupoles. The overall sequence of magnetic elements between the crossing point and the Roman pot telescope represents in fact a *powerful magnetic spectrometer* that will select protons with momentum close to the beam momentum, i.e. those which are scattered quasi-elastically in single diffraction dissociation.

The actual acceptance will depend on the specific realization of the high-β insertion.

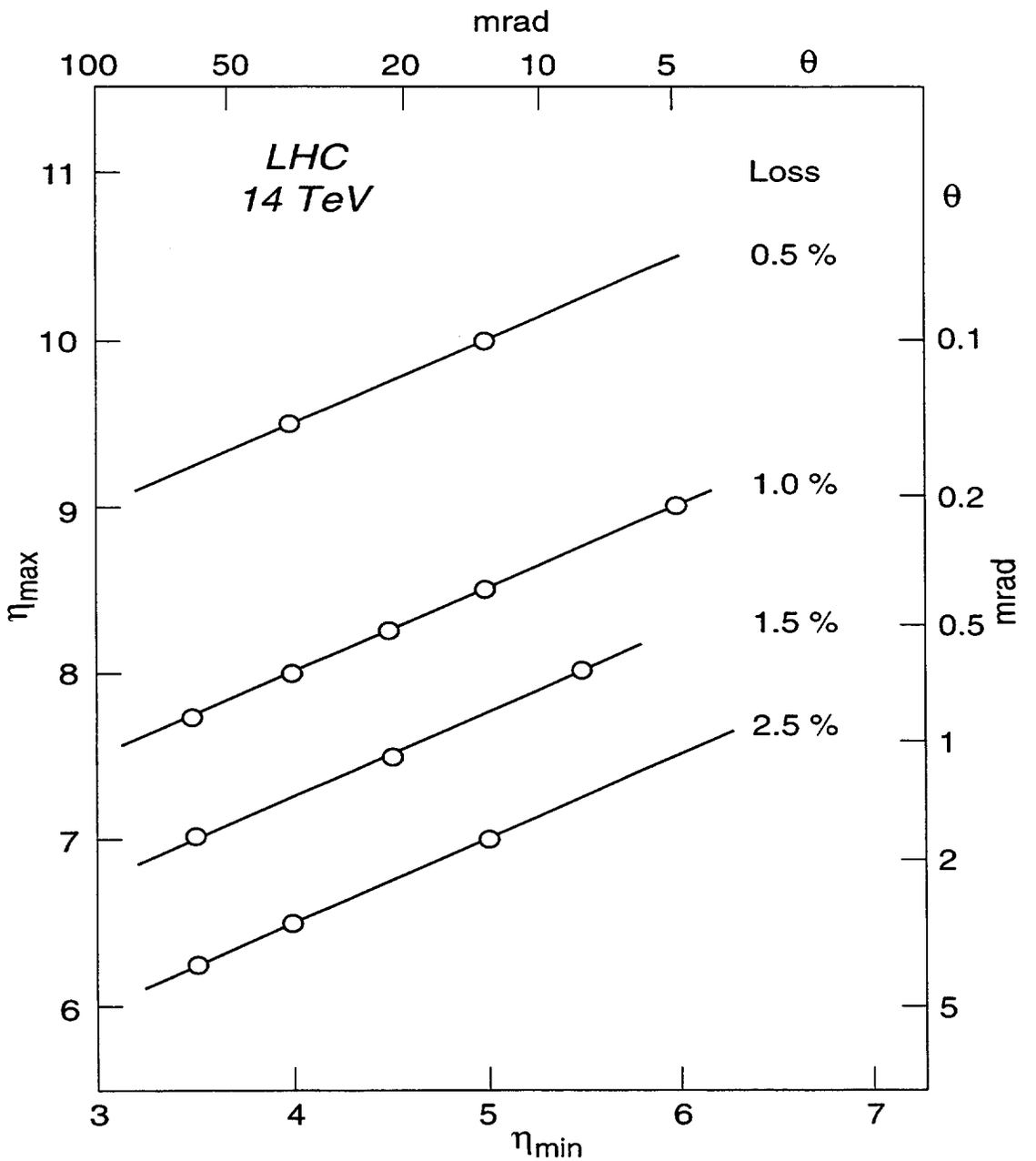

Figure 15: Results of the simulation on the efficiency of the inclusive trigger. Lines of constant fractional loss of the inelastic events are shown as functions of η_{min} and η_{max}, the extremes of the interval covered by the inelastic detector. The corresponding polar angles are also indicated.

4 Technical Aspects

4.1 The Insertion

A first feasibility study of a high-β insertion with $\beta^* = 3000$ m (the same in the horizontal and vertical plane) was made by S.Weisz[3]. A sketch of this insertion is shown in Fig.16 where the position of the Roman pots and of the inelastic detector is also shown. The behaviour of the β-function for this large β^* optics is shown in Fig.16a.

The effective distances in the vertical and in the horizontal plane are $L^V_{eff} = 65$ m and $L^H_{eff} = 53$ m.

With $y_d = 1.5$ mm, from eq.(16,17) the minimum reachable momentum transfer is $|t_{min}| = 5.2 * 10^{-2}$ GeV^2 (minimum angle of 33 μrad). This is not too far from our requirement. The maximum value of t is limited by the aperture of the quadrupole Q4 to $|t_{max}| \simeq 0.7$ GeV^2.

The same insertion could be used to measure elastic scattering at large momentum transfer without displacement of the magnetic elements, but by simple modification of the current in the quadrupoles. In fact the optics with $\beta^* = 130$ m, designed for the injection[42] (see Fig.16b) is also adequate for measuring elastic scattering at large t. The effective distances are $L^V_{eff} = 155$ m and $L^H_{eff} = 30$ m. The interval of momentum transfer which could be covered is from $|t_{min}| \simeq 0.5$ GeV^2 up to $|t_{max}| \simeq 5$ GeV^2 which is determined by the aperture of quadrupole Q2. The "Roman pots" for large-t scattering would be installed in front of quadrupole Q4.

The parameters of this insertion which are relevant for the measurement of elastic scattering are collected in Table 4 for both the high-β and medium-β mode.

β^* (m)	σ^* (mm)	σ'^* (μ rad)	L^V_{eff} (m)	L^H_{eff} (m)	ϑ_{min} (μrad)	ϑ_{max} (μrad	$\lvert t_{min}\rvert$ (GeV^2)	$\lvert t_{max}\rvert$ (GeV^2)
3000	1.2	0.4	65	53	33	120	0.052	$\simeq 0.7$
130	0.25	2.0	155	30	$\simeq 100$	$\simeq 300$	$\simeq 0.5$	$\simeq 5$

Table 4. Data on the insertion of ref.[3]. The quantities σ^* and σ'^* are the r.m.s. values of the beam radius and angular divergence

The insertion proposed in ref.[3] is only a first step toward the design of an optimized high-β insertion. It shows that with a very limited number of magnetic elements it is possible to build an insertion with properties not too far from those required by the present experiment.

Nevertheless, in spite of the fact that it is not optimized, being the only realistic study of which we are aware, we take it as a working hypothesis to fix in a first approximation the parameters of the Roman pots and associated detectors, specifically their size and spatial resolution.

The size of the detectors needed to match the angular acceptance as given in Table 5 is only of few cm^2.

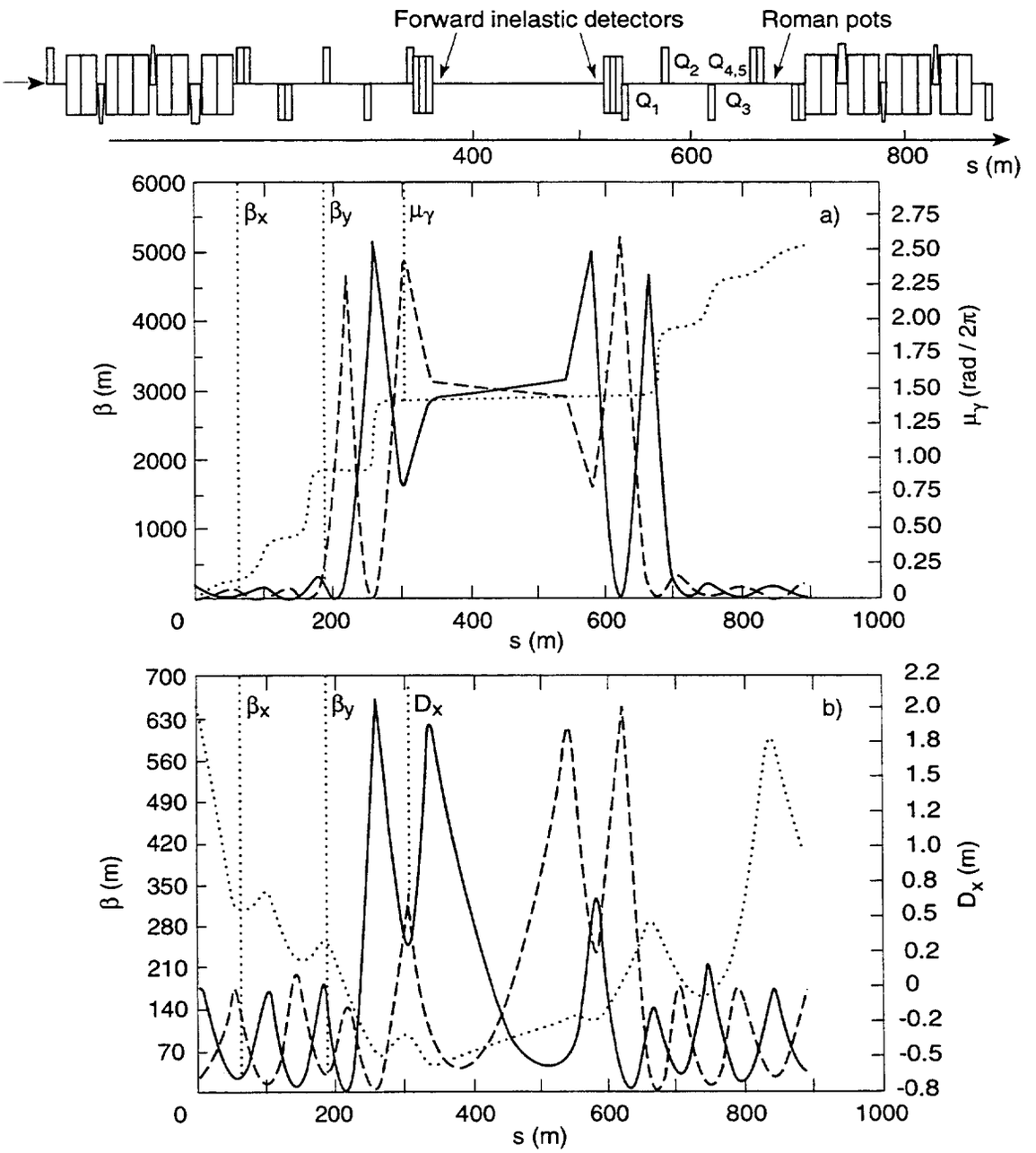

Figure 16: Sketch of the insertion designed for TOTEM by Weisz. a) Optics for low-t scattering, b) Optics for medium/large-t

4.2 Determination of the Beam Energy

As discussed in Section 3.3, the uncertainty on the beam momentum affects the measurement of σ_{tot}. In order to reduce this error to a negligible value we propose to apply the same technique which was used at the SPS Collider for the UA4/2 experiment[43]. At the SPS Collider the absolute energy of the protons was obtained by comparing the revolution frequency of protons and heavy ions.

Applying this same tecnhnique at LHC (at the time when heavy ions will be available in the LHC), the absolute energy of the circulating beams could be obtained with error less than 10^{-3}.

4.3 The Roman pots

The new Roman pots for LHC will have to be smaller than those used at the lower energy accelerators (SPS Collider and HERA). The mechanical design of the Roman pots of the Tevatron may serve as a basis for further technical developments.

It is imperative to minimize the dead space between the physical edge of the detectors and the outer edge of the pot. In addition the measurement of the actual position in space has to be very accurate.

In Fig.17 and 18 we show pictures of a Roman pot system that was designed and built at CERN[44]. The pot itself is about 6 cm wide. It has a 0.1 mm thick window whose effective area is 3 cm x 2 cm. We consider this system as a realistic starting point for the future development of the Roman pots of TOTEM.

The detectors for elastic scattering are so small (only few cm^2) that there should be no problem to attain the best spatial resolution offered by presently available technologies.

The spatial resolution is fixed by the requirement given in Section 3.1.1. Because the ultimate error on the scattering angle is determined by the intrinsic angular spread of the beams, if we accept to increase this error by $\sqrt{2}$ we have to make the contribution of the detectors equal to that coming from the beams. This condition implies

$$\Delta y^{(det)} = \Delta y^{(spot)} = L_{eff} \Delta y'^{beam} \tag{20}$$

The actual value depends on the insertion. For the high-β insertion of ref.[3] we get $\Delta y^{(det)} = 25 \mu m$. For the insertion proposed in Section 3.1.2 ($\beta^* = 1100$ m and $L_{eff} = 100$ m) we would get $\Delta^{(det)} = 65 \mu m$.

These values, however, should be considered upper limits. At present we believe that a spatial resolution of $20 \mu m$ on both the horizontal and vertical coordinates is adequate.

The main technical problem is the need for having the detectors efficient even very close to the physical edge of the detector itself. In other words the detector has to be "frameless" on one side (the side which is touching the bottom window of the Roman pot, i.e. facing the beam). This is a special and really peculiar requirement of our experiment.

At present we are considering the following options.

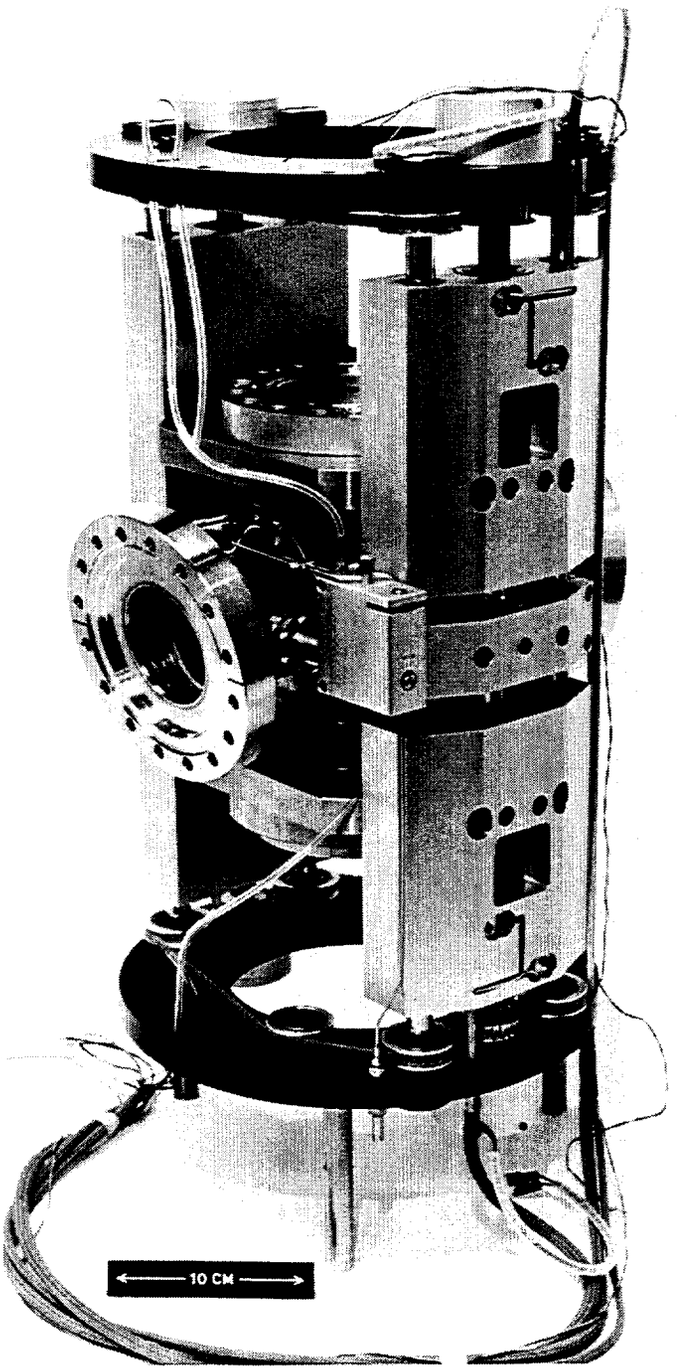

Figure 17: Picture of the overall mechanical structure of a Roman pot

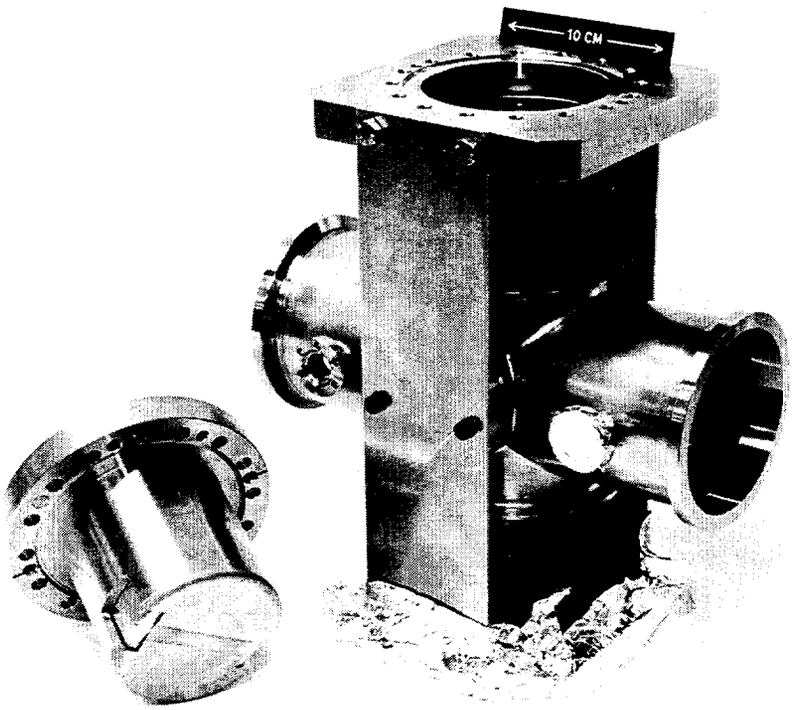

Figure 18: A Roman pot is shown together with the special short section of vacuum chamber equipped with bellows

- Silicon detectors with (x,y) strips or (x,y,u) strips.
- Silicon detectors with combination of pads and strips.
- Hodoscopes of scintillating fibers of the UA4/2 type[45].

Of crucial importance for a Roman pot experiment is the control of the absolute geometrical alignment of facing detectors (up-down). The final systematic error depends on that measurement and on the uncertainty on the beam momentum. We need an absolute uncertainty less than $10\mu m$.

4.4 The Forward Inelastic Detector

We design the *forward inelastic detector* according to the following requirements.

- Fully inclusive trigger also for single diffractive events with expected loss on N_{inel} at the 1% level (left-right trigger and single arm trigger are foreseen)
- Capability of reconstruction of the collision vertex in order to disentangle beam-beam events from background.

Following the discussion in Section 3.3.1 , we choose the pseudorapidity coverage from η_{min}= 5 up to η_{max} = 8.5 which corresponds to the range of polar angles from about 0.5 mrad up to 13 mrad. For this angular range, the Monte Carlo simulation (see Fig.15) indicates that the loss of inelastic events is at the 1% level. The results of the simulation are listed in Table 5 for both non diffractive (NSD) and single diffractive (SD) events and for both trigger combinations.

	Left-right	Single arm
NSD	0.99	1.00
SD	0.20	0.93

Table 5. Monte Carlo efficiencies of the left-right trigger and single arm trigger for NSD and SD events at LHC. The covered pseudorapidity interval is from η_{min}= 5 up to η_{max} = 8.5. It was assumed $\sigma_{SD}/\sigma_{inel}$ = 0.14.

The simulation also shows that the average number of charged tracks per event in this angular range is about 15 on each side. Therefore with a reference luminosity for the high-β insertion of $10^{28} cm^{-2} s^{-1}$, we expect on the average about 10^4 charged particles/s traversing each telescope. It is clear that for the TOTEM operation there is no problem of rate or radiation damage.

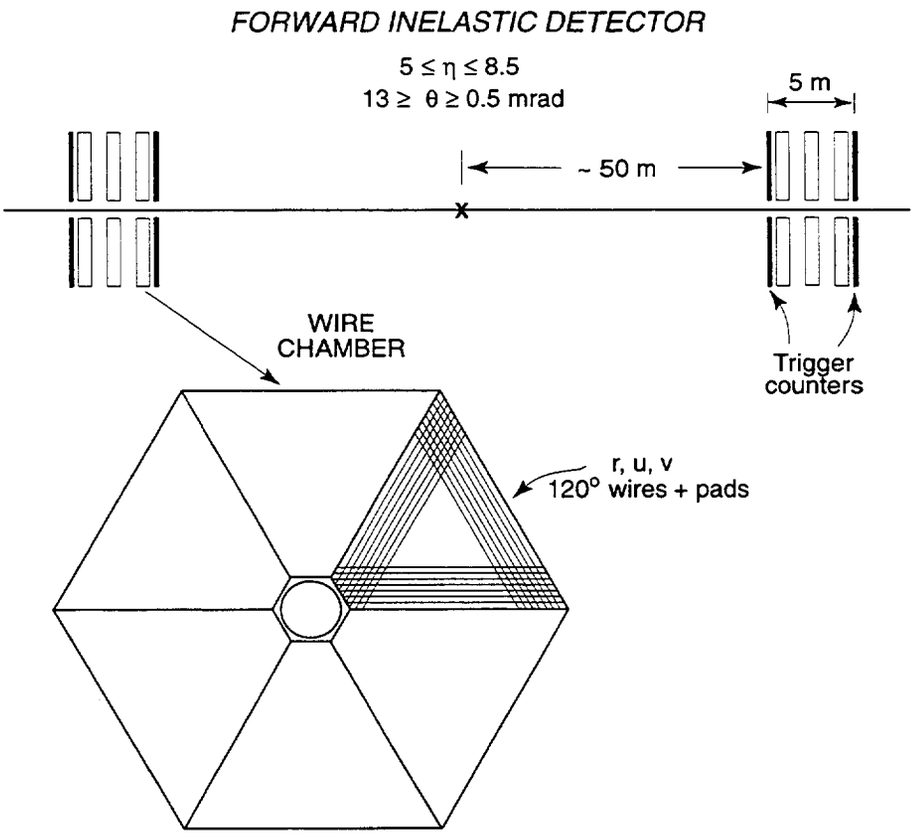

Figure 19: Layout of the forward inelastic detector

A possible layout is shown in Fig.19. Each arm consists of a telescope of two planes of scintillation counters placed 5 m apart with 3 gas chambers in between. Each telescope will be placed at about 50 m from the crossing. The shape of each detector could be hexagonal with inner radius of 2.5 cm and outer radius of about 65 cm. The distance from the crossing point is determined by the minimum polar angle and by the radius of the standard vacuum chamber (2.2 cm).

The scintillation counters of each telescope will be able to discriminate outgoing from ingoing particles by timing. The gas chambers will provide reconstruction of the charged particle tracks and extrapolation to the collision point.

The basic requirement for the gas chambers is a resolution of few tenths of mm. Taking into account the lever arm, this will allow extrapolation to the centre of the intersection region with an error on the transverse coordinate of few mm which is sufficient.

It is clear that there is no severe condition on the gas chambers, neither from the expected rate nor from the required spatial resolution. We will therefore choose detectors of a type which is easy to build and with reliable and inexpensive electronics.

A possible choice is given by the "Thin Gap Gas Chambers" operated in the high gain mode[46]. These chambers have been used in the OPAL experiment at LEP. Each chamber would consist of 6 trapezoidal units (actually truncated equilateral triangles) with azimuthal acceptance of 60^0.

The wires of the anode plane (with separation of 1.5 - 2 mm) run normally to the radial direction. On the two cathode planes there would be strips with about 2 mm pitch running in the u and v directions at angles of 120^0 to the anode wires. Each chamber provides the coordinate of the tracks with redundancy of one additional plane[47].

4.5 Background and Radiation Damage

4.5.1 Background in the Roman pots

The "Roman" pots are sufficiently away from the crossing point not to be affected by the background coming from beam-beam interactions. The main source of background is induced by the protons in the machine (beam-gas, beam scattering in low aperture parts upstream). This background was of course extensively studied by the LHC Study Group[38].

A detailed simulation discussed by B.Jeanneret[48] gives the background profile as a function of the distance from the beam axis. The results of this calculation, shown in Fig.20, demonstrate the effectiveness of the collimators in reducing the background rate at distances from the beam axis above $10 \times \sigma_{beam}$.

At nominal intensity, the average loss in one ring all around the machine should be about 3×10^9 protons s^{-1}. If this loss is uniformly distributed around the ring the local loss is about 10^5 protons m^{-1} s^{-1}. The collimators are expected to provide a reduction factor of about 100.

Therefore, assuming the closest part of the pot placed at a distance of $15 \times \sigma_{beam}$, this would lead to a background rate of the order of magnitude of 10^3 Hz as seen by the detectors at the maximum beam intensity. This rate is very similar to that observed during the UA4/2 run and can be easily faced by the TOTEM experiment. It will be further lowered by the bunch reduction factor during the total cross section measurement.

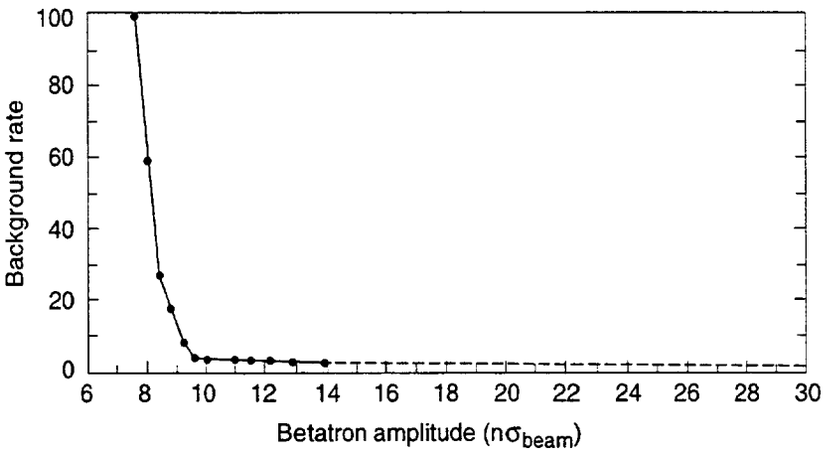

Figure 20: Expected background as a function of the distance from the beam axis

4.5.2 Background in the inelastic detector

Contrary to what is expected for the Roman pots, the background in the "inelastic" detector is mainly induced by the showering of the very forward particles produced in beam-beam interactions.

At a luminosity of 10^{28} cm^{-2} s^{-1}, the average number of interactions will be 1000 Hz, i.e. 10^{-2} interactions per crossing at reduced number of bunches. The measurement will not be affected by multiple interactions during the same crossing.

The background comes essentially from beam-gas events simulating Single Diffractive (SD) events. For the total cross section measurement assuming the luminosity given above and reduced intensity, the ratio of SD to background events in the interaction region is about 10. With this factor the SD rate could also be determined with sufficient precision to get the inelastic cross section at the 1% level. On the other hand the ratio of the SD events to all inelastic could be determined at higher luminosity, thus lowering the background.

From the previous discussion on the expected rates, it is clear that for the TOTEM operation we do not expect problems of radiation damage.

4.6 Data Acquisition

The average event rate and data flow generated by the TOTEM detector for each type of event is given in Table 6:

	$Events/sec\ at\ L = 10^{28} cm^{-2} s^{-1}$	Event size
Elastic Events	$\simeq 300$	$\simeq 5$ kBytes
Inelastic Events	$\simeq 800$	$\simeq 50$ kBytes

Table 6. The average event rate and event size of TOTEM

These numbers are based on experience gained at the SPS Collider scaled to the LHC multiplicities. Using a prescaling factor of 10 for the inelastic type of events and a nominal luminosity of 10^{28} cm^{-2} sec^{-1} for the total cross section measurement, the data flow will be about 5.5 MBytes sec^{-1}.
This data flow can be achieved with present technologies without any problem. As an example, a possible scheme, the one used in the CMS calorimeter test beam and maintained by some of us, is shown in Fig.21. The TOTEM experiment doesn't aim at developing a specific data acquisition system and will benefit from the technologies of the main LHC experiments.

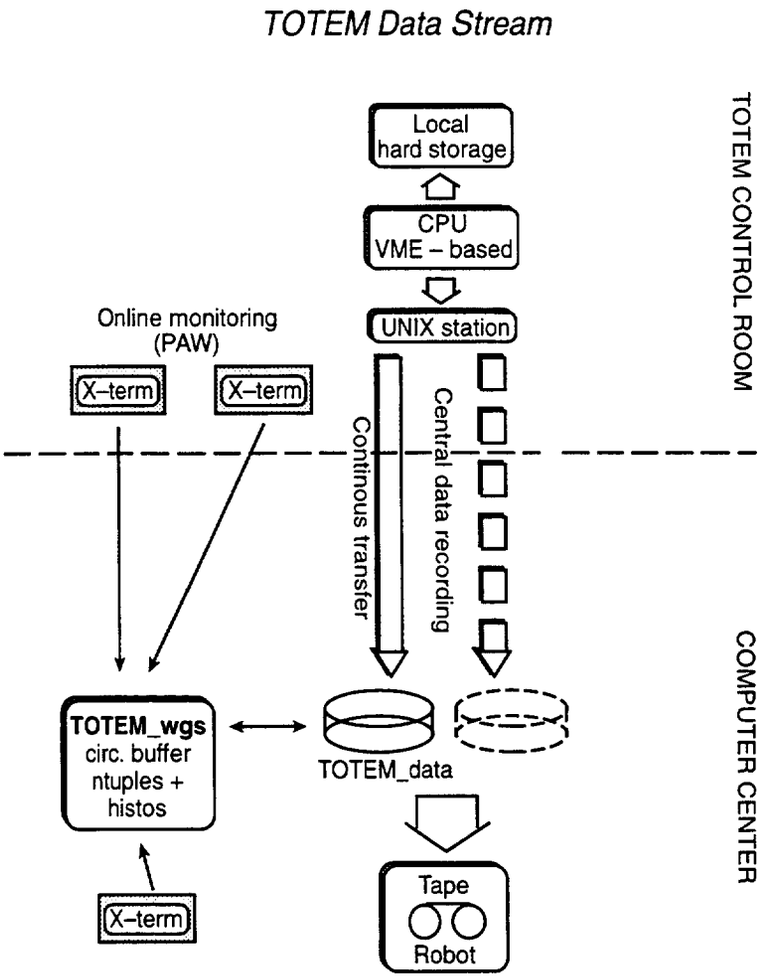

Figure 21: Scheme of the data acquisition system

5 Conclusions

In this Letter of Intent we have discussed the physics motivations for the measurement of fundamental properties of the hadronic interactions at LHC, the highest energy accelerator which will be available in the next decade.
Our experimental programme consists of the following measurements:

- Total cross section
- Elastic scattering
- Diffraction dissociation

The experimental methods proposed are certainly realistic because of the *know-how* gained in previous experiments at lower energy accelerators. From our previous experience we are confident that the extrapolations up to the LHC energy are correct.

Our first objective is the measurement of the total cross section which implies a measurement of elastic scattering at low-t and of diffraction dissociation.

This measurement fits well with the running-in period of the accelerator when the luminosity is presumably quite low but still sufficient for studying low momentum transfer processes.

At a later stage, we plan to study large-t elastic scattering and investigate the Coulomb scattering.

We have not discussed the cost of the experiment because it is certainly quite modest and in addition this would be premature at this early stage. We expect, however, that the cost of the detectors and associated electronics will be supported mostly by the external institutions.

6 Acknowledgments

This experiment is intimately linked with the machine. In particular the optics of the insertion and the collimation system are of crucial importance for this experiment.
This Letter of Intent couldn't have been written without the contribution of J.M. Deconto, J. Gareyte, B. Jeanneret and T. Linnecar. We wish to thank all of them very warmly. Special thanks are due to R. Maleyran for very useful discussions on the mechanics of the Roman pots and to J. Camas and M. Sillanoli for a demonstration.

References

[1] M.Bozzo et al., Expression of Interest, Proceedings of the General Meeting on LHC Physics and Detectors, Evian 1992, pag. 751.

[2] The TOTEM Collaboration, CERN/LHCC 93-47, 14 September 1993.

[3] S.Weisz, CERN preprint SL-Note 94-09 (AP).

[4] The TOTEM Collaboration, CERN/LHCC 94-39, 19 October 1994.

[5] C.Augier et al., Phys. Lett. B315 (1993) 503.

[6] M.Bozzo et al., Phys. Lett. 147B (1984) 392.

[7] G.J.Alner et al., Z. Phys. C32 (1986) 153.

[8] N.A.Amos et al., Phys. Lett. 243B (1990) 158 and
Phys. Rev. Lett. 68 (1992) 2433.

[9] F.Abe et al., Phys. Rev. D, 50 (1994) 5550.

[10] C.Augier et al., Phys. Lett. B316 (1993) 448.

[11] R.M.Baltrusaitis et al., Phys. Rev. Lett. 52 (1984) 1380.
M.Honda et al., Phys. Rev. Lett. 70 (1993) 525.

[12] M.Froissart, Phys. Rev. 123 (1961) 1053.
A.Martin, Nuovo Cimento 42 (1966) 930.

[13] C.Bourrely, J.Soffer and T.T.Wu, Nucl. Phys. B247 (1984) 15 and
Z. Phys. C37 (1988) 369.

[14] A.Donnachie and P.V.Landshoff, Phys. Lett. B296 (1992) 227.

[15] N.N.Khuri and T.Kinoshita, Phys. Rev. 137 (1965) B720.

[16] U.Amaldi et al., Phys. Lett. 66B (1977) 390.

[17] N.A.Amos et al., Nucl. Phys. B262 (1985) 689.

[18] N.N.Khuri, Proc. of the "Rencontres de Physique de la Vallée d'Aoste", La Thuile 1994, pag. 701 and
Proc. of the VIIth "Rencontres de Blois", Blois 1995, pag.471.

[19] H.Cheng and T.T.Wu, Phys. Rev. Lett. 24 (1970) 1456 and
"Expanding Protons - Scattering at High Energies", Cambridge 1987.

[20] G.Barbiellini et al., Phys. Lett. B39 (1972) 663.

[21] M.Bozzo et al., Phys. Lett. 147B (1984) 385.

[22] N.A.Amos et al., Phys. Lett. B247 (1990) 127.

[23] P.Gauron, B.Nicolescu and O.V.Selyugin, Phys. Lett. B397 (1997) 305.

[24] A.Martin, CERN preprint TH 97-23.

[25] E.Nagy et al., Nucl. Phys. B150 (1979) 221.

[26] A.Breakstone et al., Phys. Rev. Lett. 54 (1985) 2180.

[27] M.Bozzo et al., Phys. Lett. 155 (1985) 197.

[28] A.Donnachie and P.V.Landshoff, Z. Phys. C2 (1979) 55,
Nucl. Phys. B267 (1986) 690 and preprint DAMPT 96/66, M/C-TH 96/22.

[29] V.N.Gribov, Proc. of the 1960 Int. Conf. on High-Energy Physics, Rochester, 1960, pag.340.

[30] C.Bourrely and J.Soffer (private communication).

[31] P.Desgrolard, M.Giffon and E.Predazzi, Z. Phys. C63 (1994) 241
P.Desgrolard and M.Giffon (private communivation).

[32] M.L.Good and W.D.Walker, Phys. Rev. 120 (1960) 1857.

[33] J.C.M.Armitage et al., Nucl. Phys. B194 (1982) 365 and refs. therein.

[34] D.Bernard et al., Phys. Lett. B186 (1987) 227.

[35] F.Abe et al., Phys. Rev.D50 (1994) 5535.

[36] M.Bozzo et al., Phys. Lett. B136 (1984) 217.

[37] M. Haguenauer and G. Matthiae, Proc. of the ECFA - CERN Workshop on the Large Hadron Collider in the LEP Tunnel, Lausanne 1984, vol. 1, pag. 303.

[38] *The Large Hadron Collider* - Conceptual Design CERN/AC/95-05(LHC), Section 2.9, 3.6 and 4.

[39] A.Verdier, LHC Project Note 93 (1997)

[40] J.Gareyte (private communication)

[41] T.Sjostrand, Computer Physics Commun. 82 (1994) 74 and
CERN-TH, 7112/93.

[42] S.Weisz (private communication)

[43] X.Altuna et al., CERN/SL/92-32 (1992)

[44] J.Camas and M.Sillanoli (private communication)

[45] C.Augier et al., Nucl. Instr. and Methods A389 (1997) 409.

[46] S.Majewski, G.Charpak, A.Breskin and G.Mikenberg, Nucl. Instr. and Methods 217 (1983) 265.

[47] W.Adam et al., (Genova University preprint, 1997)

[48] I.Ajguirei, J.Baïchev, B.Jeanneret, V.Talamov and A.Uzumian, Workshop on LHC background, CERN, March 1996, K. Potter editor.